

Supporting Information

An experimentally validated QSAR model for surface pKa prediction of heterolipid having potential as delivery materials for nucleic acid therapeutics

Dinesh M. Dhumal¹, Pankaj D. Patil³, Raghavendra V. Kulkarni⁴, Krishnacharya G. Akamanchi¹,

2*

¹Department of Pharmaceutical Sciences and Technology, Institute of Chemical Technology, Matunga (E), Mumbai 400019, India.

²Department of Allied Health Sciences, Shri B.M. Patil Medical College, Hospital and Research Centre, BLDE Deemed to be University, Vijayapura, India 586 103

³Department of Chemistry, Syracuse University, Syracuse, NY 13244, United States.

⁴BLDEA's SSM College of Pharmacy & Research Centre, Vijayapura, India 586 103.

***Corresponding author:** Krishnacharya Akamanchi; E-mail: kgap@rediffmail.com;

Fax: +91-22-33611020; Tel: +91-22-33612214

Materials and methods	4
Calculation of molecular descriptor	5
Generation of training and test sets	5
Forward Stepwise as variable selection method	5
2D-QSAR model development	6
Model validation and evaluation	6
Table S1: Structures of heterolipids with corresponding experimental pKa values	9
Table S2: Selected descriptors for 2D-QSAR modeling of pKa activity of heterolipids	12
Table S4: Correlation matrix between the physicochemical descriptors and alignment independent descriptor influencing the pKa	15
Table S5: Comparative data of experimental and predicted pKa of heterolipids	16
Synthesis of Heterolipids	18
Scheme 1: Synthesis of Series-I bicephalous single tail heterolipids	18
Scheme II: Synthesis of series-II lysine based monocephalous two tail heterolipids.	25
Figure S1: ¹H NMR spectra of (Z)-bis(2-(dimethylamino)ethyl) 3,3'-((2-(oleoyloxy)ethyl)azanediyl)dipropoanoate 7a (HL-22)	30
Figure S2: ¹³C NMR spectra of (Z)-bis(2-(dimethylamino)ethyl) 3,3'-((2-(oleoyloxy)ethyl)azanediyl)dipropoanoate 7a (HL-22)	31
Figure S3: High resolution mass spectrum in electrospray positive mode of (Z)-bis(2-(dimethylamino)ethyl) 3,3'-((2-(oleoyloxy)ethyl)azanediyl)dipropoanoate 7a (HL-22)	32
Figure S4: ¹H NMR spectra of (Z)-bis(2-(dimethylamino)ethyl)3,3'-((3(oleoyloxy)propyl)azanediyl)dipropoanoate 7b (HL-32)	33
Figure S5: ¹³C NMR spectra of (Z)-bis(2-(dimethylamino)ethyl)3,3'-((3(oleoyloxy)propyl)azanediyl)dipropoanoate 7b (HL-32)	34
Figure S6: High resolution mass spectrum in electrospray positive mode of the (Z)-bis(2-(dimethylamino)ethyl)3,3'-((3(oleoyloxy)propyl)azanediyl)dipropoanoate 7b (HL-32)	35
Figure S7: ¹H NMR spectra of (Z)-bis(3-(dimethylamino)propyl)3,3'-((2(oleoyloxy)ethyl)azanediyl)dipropoanoate 7c (HL-23)	36
Figure S8: ¹³C NMR spectra of (Z)-bis(3-(dimethylamino)propyl)3,3'-((2(oleoyloxy)ethyl)azanediyl)dipropoanoate 7c (HL-23)	37
Figure S9: High resolution mass spectrum in electrospray positive mode of (Z)-bis(3-(dimethylamino)propyl)3,3'-((2(oleoyloxy)ethyl)azanediyl)dipropoanoate 7c (HL-23)	38
Figure S10: ¹H NMR spectra of (Z)bis(3(dimethylamino)propyl)3,3'((3(oleoyloxy)propyl)azanediyl)dipropoanoate 7d, (HL-33)	39

Figure S11: ¹³C NMR spectra of	
(Z)bis(3(dimethylamino)propyl)3,3'((3(oleoyloxy)propyl)azanediyl)dipropanoate 7d (HL-33)40
Figure S12: High resolution mass spectrum in electrospray positive mode of	
(Z)bis(3(dimethylamino)propyl)3,3'((3(oleoyloxy)propyl)azanediyl)dipropanoate 7d (HL-33)41
Figure S13: ¹H NMR of (R)-2, 6-dioleamidohexanoic acid 1042
Figure S14: ¹³C NMR of (R)-2, 6-dioleamidohexanoic acid, 1043
Figure S15: Mass of (R)-2, 6-dioleamidohexanoic acid, 1044
Figure S16: ¹H NMR (R)-2-(dimethylamino)ethyl 2,6-dioleamidohexanoate 12a (HLys E2)45
Figure S17: ¹³C NMR (R)-2-(dimethylamino)ethyl 2,6-dioleamidohexanoate 12a (HLys E2)46
Figure S18: High resolution mass spectrum of (R)-2-(dimethylamino)ethyl 2,6-dioleamidohexanoate 12a (HLys E2).47
Figure S19: ¹H NMR (R)-3-(dimethylamino)propyl 2,6-dioleamidohexanoate 12b48
Figure S20: ¹³C NMR (R)-3-(dimethylamino)propyl 2,6-dioleamidohexanoate 12b (HLys E3)49
Figure S21: High resolution mass of (R)-3-(dimethylamino)propyl 2,6-dioleamidohexanoate 12b (HLys E3)50
Figure S22: ¹H NMR (Z)-N,N'-((R)-6-((2-(dimethylamino)ethyl)amino)-6-oxohexane-1,5-diyl)dioleamide 12c (HLys A2)51
Figure S23: ¹³C NMR (Z)-N,N'-((R)-6-((2-(dimethylamino)ethyl)amino)-6-oxohexane-1,5-diyl)dioleamide 12c (HLys A2)52
Figure S24: High resolution mass spectrum of (Z)-N,N'-((R)-6-((2-(dimethylamino)ethyl)amino)-6-oxohexane-1,5-diyl)dioleamide 12c (HLys A2)53
Figure S25: ¹H NMR (Z)-N,N'-((R)-6-((3-(dimethylamino)propyl)amino)-6-oxohexane-1,5diyl)dioleamide 12d (HLysA3)54
Figure S26: ¹³C NMR (Z)-N,N'-((R)-6-((3-(dimethylamino)propyl)amino)-6-oxohexane-1,5diyl)dioleamide 12d (HLysA3)55
Figure S27: High resolution mass spectrum (Z)-N,N'-((R)-6-((3-(dimethylamino)propyl)amino)-6-oxohexane-1,5diyl)dioleamide 12d (HLysA3)56
Figure S28: Particle size of LNP'S57
Figure S29: Correlation between predicted and experimental pKa58
References59

Materials and methods

Materials

Oleic acid (Technical grade, 90%), 2-dimethylaminoethanol, 3-dimethylamino-1-propanol, cholesterol, 6-(p-toluidino)-2-naphthalenesulfonic acid sodium salt (TNS), cholesterol distearoylphosphatidylcholine(DSPC) and MPEG-2000-DSPE sodium salt were purchased from Sigma-Aldrich (USA). Acryloyl chloride was obtained from Alfa Aesar (USA). 3-Amino-1-propanol, ethanolamine, 4-dimethylaminopyridine (DMAP), 1-hydroxybenzotriazole (HOBT) was obtained from Spectrochem (India). Triethylamine (TEA) and thionyl chloride were obtained from S. D. Fine Pvt. Ltd. (India). 1-(3-Dimethylaminopropyl)-3-ethyl carbodiimide hydrochloride (EDAC) was purchased from Sisco Research Laboratories Pvt. Ltd (India). Dichloromethane (DCM), tetrahydrofuran (THF) and other solvents used were of an analytical grade. Precoated Silica-gel 60F₂₅₄ plates used for thin layer chromatography (TLC) to monitor reactions were obtained from Merck. Water used in the entire study was obtained from the Milli-Q water purification system of Millipore Corporation (Bedford, USA).

Instrumentation

The molecular modelling studies were performed on Acer computer having Intel core i3 2310 M Processor and Windows 7 operating system using the molecular modeling software VLife MDS (Molecular Design Suite)TM 4.3 supplied by VLife Sciences Technologies Pvt. Ltd., Pune, India. Infrared (IR) spectra were recorded on Shimadzu IRAffinity-1S ATIR model with IRsolution software. ¹H NMR and ¹³C NMR spectra were recorded on Agilent Technologies MR - 400 nuclear magnetic resonance spectrometer/ Bruker Advance III 400 at frequencies 400 MHz and 100 MHz respectively. The HRMS analysis was carried out with a SYNAPT G2 HDMS (Waters) mass spectrometer equipped with a pneumatically assisted atmospheric pressure ionization (API) source. The sample was ionized in positive electrospray mode under the following conditions: electrospray voltage: 2.8 kV; orifice voltage: 20 V; Nebulization gas flow (nitrogen): 100 L / h. The high-resolution mass spectrum (MS) was obtained with a flight time analyzer (TOF). The exact mass measurement was done in triplicate with an external calibration. The sample is dissolved in 300 µl of methanol and then diluted 1/10 in a 1% solution of methanol formic acid. The solution of the extract is introduced into the infusion ionization source at a flow rate of 10.0 µl / min.

Calculation of molecular descriptor¹

2D-QSAR study requires the calculation of molecular descriptors. A large number of 2D physicochemical individual descriptors such as Mol. Wt., Volume, Rotatable Bond Count, Xlog P, Slog P, smr, polarizability AHC, polarizability AHP; Baumann alignment independent topological descriptors type have been computed for these cleaned and 3D optimized heterolipids referred to above with a view to develop structure-activity relationship of heterolipids against pKa. A total of 131 descriptors were calculated by QSAR Plus module within VLife Sciences Molecular Design Suite which was subsequently reduced to 116. The pre-processing of the independent variables (i.e., descriptors) was done by removing invariable (constant column) as they do not contribute to the QSAR.

Generation of training and test sets

From the 56 molecules, 50 molecules were considered, as remaining 6 molecules eliminated as outliers, these are 2, 5, 43, 50, 51 and 52. The molecules were divided manually into a training set (38 molecules) for generating 2D QSAR models and a test set (12 molecules) for validation of the developed model. Selection of the training set and test set was done in order to assess the similarity of the distribution pattern of the compounds in the generated sets, statistical parameters (with respect to the activity) i.e. mean, maximum, minimum and standard deviation were calculated for the training and test sets. For selection of training and test set, we ensured that the molecules have uniform spread (training and test) in terms of both activity and chemical space. Thus, the test set is truly representative of the training set. This approach resulted in selection of molecules 7, 8, 17, 22, 26, 29, 33, 34, 41, 45, 47 and 49 as the test set and the remaining 38 molecules as the training set.

Forward Stepwise as variable selection method

To, select a subset of descriptors (variables) from the descriptor pool, a variable selection method like forward stepwise is required. In SW forward variable selection algorithm, the search procedure begins with developing a trial model step by step with a single independent variable and to each step, independent variables are added one at a time, examining the fit of the model by using different QSAR methods. Thus, the model is repeatedly altered from the previous one by adding

or removing a predictor variable in accordance with the ‘stepping criteria’ (in this case, $F = 4$ for inclusion for the forward selection method). The method continues until there is no more significant variable remaining outside the model.

In the selected equations, the cross-correlation limit was set at 0.5, the number of variables at 10 and the term selection criteria at r^2 . An F value was specified to evaluate the significance of a variable. The variance cut-off was set at 0.0, and scaling as none.

2D-QSAR model development

Partial Least Squares (PLS) Regression Method²

PLS is an effective technique for finding the relationship between the properties of a molecule and its structure. In mathematical terms, PLS relates a matrix Y of dependent variables to a matrix X of molecular structure descriptors, i.e., a latent variable approach to modeling the covariance structures in these two spaces. PLS have two objectives: to approximate the X and Y data matrices, and to maximize the correlation between them. Whereas the extraction of PLS components is performed stepwise and the importance of a single component is assessed independently, a regression equation relating each Y variable with the X matrix is created. PLS decomposes the matrix X into several latent variables that correlate best with the activity of the molecules. PLS can be done using NIPALS or SIMPLS iterative algorithm, with consecutive estimates obtained using the residuals from previous iterations as the new dependent variable

The QSAR model was developed using partial least squares by forward variable selection method with pKa activity field as dependent variable and 116 physicochemical descriptors as independent variable having cross correlation limit of 0.5. Selection of test and training set was done by manually.

Despite its wide acceptance, a high value of q^2 alone is an insufficient criterion for a QSAR model to be highly predictive. Use of greater number of descriptors particularly requires the model to be validated by external predictive power (r^2 predictive). Hence a set of 12 molecules covering different heterolipids were employed as test to evaluate the predictivity of training set.

Model validation and evaluation³

This is done to test the internal stability and predictive ability of the QSAR models.

A) Internal validation

Internal validation was carried out using leave-one-out (q^2 , LOO) method. To calculate q^2 , each molecule in the training set was sequentially removed, the model refit using same descriptors, and the biological activity of the removed molecule predicted using the refit model. The q^2 was calculated using Eq.1

$$q^2 = 1 - \frac{\sum (y_{i\text{actual}} - y_{i\text{pred}})^2}{\sum (y_i - y_{\text{mean}})^2} \quad \text{Eq. 1}$$

Where $y_{i\text{actual}}$ and $y_{i\text{pred}}$ are the actual and the predicted activity of the i^{th} molecule in the training set, respectively, and y_{mean} is the average activity of all molecules in the training set.

B) External validation

For external validation, activity of each molecule in the test set was predicted using the model generated from the training set. The $\text{pred_}r^2$ value is calculated as follows (Eq. 2)

$$\text{pred_}r^2 = 1 - \frac{\sum (y_{i\text{actual}} - y_{i\text{pred}})^2}{\sum (y_i - y_{\text{mean}})^2} \quad \text{Eq. 2}$$

Where $y_{i\text{actual}}$ and $y_{i\text{pred}}$ are the actual and the predicted activity of the i^{th} molecule in the test set, respectively, and y_{mean} is the average activity of all the molecules in the training set

C) Randomization test

To evaluate the statistical significance of a QSAR model for an actual data set, one tail hypothesis testing was used. The robustness of the models for training set was examined by comparing these models to those derived for random data sets. Random sets were generated by rearranging the activities of the molecules in the training set and the significance of the models was derived based on the calculated Z score; (Eq. 3.3).

$$Z_{\text{score}} = \frac{(q^2_{\text{org}} - q^2_{\text{a}})}{q^2_{\text{std}}} \quad \text{Eq. 3}$$

Where q^2_{org} is the q^2 value calculated for the actual data set, q^2_a is the average q^2 , and q^2_{std} is the standard deviation of q^2 , calculated for various iterations using different random data sets. The probability (α) of significance of the randomization test is derived by using calculated Z score value as given in the literature.

D] Evaluation of the quantitative model⁴

Developed quantitative model was evaluated using following statistical measures: squared correlation coefficient r^2 , q^2 , cross-validated r^2 (by LOO) which is relative measure of quality of fit; $pred_r^2$, r^2 for external test set; r^2_se , standard error of squared correlation coefficient; q^2_se , standard error of cross-validation; $pred_r^2_se$, standard error of external test set prediction; Fischer's value F-test which represents F-ratio between the variance of calculated and observed activity; N, number of observations (molecules) in the training set; Z score, the Z score calculated by q^2 in the randomization test; $best_rand_q^2$, the highest q^2 value in the randomization test and $alpha_rand_q^2$, the statistical significance parameter obtained by randomization test. The calculated value of F-test when compared with tabulated value of F-test shows the level of statistical significance (99.99%) of the QSAR model. The low standard error of $pred_r^2se$, q^2_se and r^2_se shows absolute quality of fitness of the model. The generated QSAR model was validated for predictive ability inside the model by using cross validation (LOO) for q^2 and external validation, which is more robust alternative method by dividing the data into training set & test set and calculating $pred_r^2$. The high $pred_r^2$ and low $pred_r^2_se$ were show high predictive ability of the model. The r^2 , q^2 and $pred_r^2$ values were used as deciding factors in selecting the optimal model.

Table S1: Structures of heterolipids with corresponding experimental pKa values

Sr no	Compounds	pKa	Sr no	Compounds	pKa
1		6.68	29		7.03
2		5.97	30		6.17
3		5.94	31		5.44
4		6.65	32		7.88
5		6.79	33		7.25
6		6.42	34		7.61
7		6.43	35		6.49
8		7.29	36		6.52
9		6.98	37		7.62
10		6.73	38		7.31

11		5.65	39		6.62
12		5.6	40		8.02
13		6.85	41		8.11
14		4.17	42		7.23
15		5.64	43		6.08
16		6.44	44		7.21
17		6.93	45		7.07
18		7.16	46		5.5
19		6.95	47		6.21
20		6.78	48		8.12
21		6.77	49		7.57

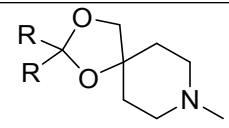
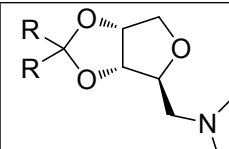
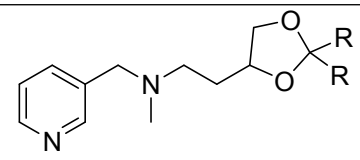
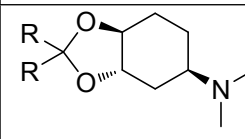
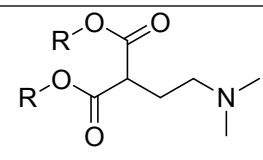
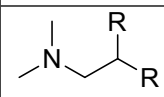
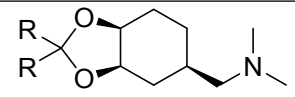
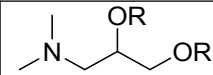
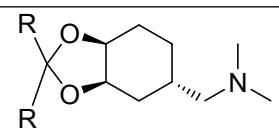
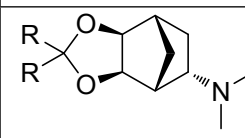
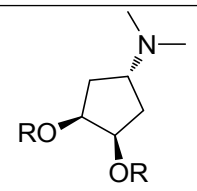
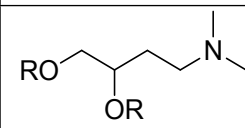
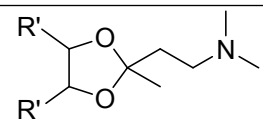
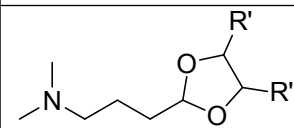
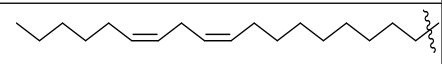
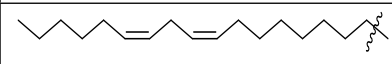
22		6.53	50		6.87
23		4.95	51		5.49
24		6.66	52		5.73
25		6.6	53		6.38
26		6.65	54		6.63
27		7.73	55		7.27
28		6.6	56		6.91
R			R'		

Table S2: Selected descriptors for 2D-QSAR modeling of pKa activity of heterolipids

Sr. No.	Descriptors	Description
1	T_N_O_3	T_N_O_3 is a count of number of nitrogen atoms (single, double or triple bonded) separated from any oxygen atom (single or double bonded) by three bonds in a molecule
2	H-Donor Count (HDC)	Number of hydrogen bond donor atoms
3	T_2_C_0	T_2_C_0 is the count of number of double bounded atoms (i.e. any double bonded atom, T_2) separated from Carbon atom by zero bond.
4	X log P	This descriptor signifies ratio of solute concentration in octanol & water and generally termed as Octanol/Water partition Coefficient.
5	T_N_O_7	T_N_O_7 is a count of number of nitrogen atoms (single, double, or triple bonded) separated from any oxygen atom (single or double bonded) by seven bonds in a molecule
6	T_N_N_3	T_N_N_3 is a count of number of nitrogen atoms (single, double, or triple bonded) separated from any nitrogen atom (single or double bonded) by three bonds in a molecule
7	T_O_O_2	T_O_O_2 is a count of number of oxygen atoms (single, double, or triple bonded) separated from any oxygen atom (single or double bonded) by two bond distance in a molecule
8	Rotatable Bond Count (RBC)	Number of rotatable bonds
9	T_N_O_4	T_N_O_4 is a count of number of nitrogen atoms (single, double, or triple bonded) separated from any oxygen atom (single or double bonded) by four bonds in a molecule
10	T_O_O_4	T_O_O_4 is a count of number of oxygen atoms (single, double or triple bonded) separated from any oxygen atom (single or double bonded) by four bond distance in a molecule

Table S3: Selected physicochemical and alignment independent descriptors used in 2D-QSAR model with values

Molec uleID	Selected Descriptors										
	Expt. pKa	T_N_ O_3	HD C	T_2_ C_0	XlogP	T_N_ O_7	T_N_ N_3	T_O_ O_2	RB C	T_N_ _O_ 4	T_O_ O_4
1	6.68	0	0	8	13.436	0	0	1	37	1	0
3	5.94	1	0	8	12.986	0	0	1	36	1	0
4	6.65	0	0	8	13.436	0	0	1	37	1	0
6	6.42	0	0	8	13.648	0	0	1	35	2	0
7	6.43	0	0	8	13.648	0	0	1	35	2	0
8	7.29	0	0	8	14.098	0	0	1	35	1	0
9	6.98	0	0	8	14.098	0	0	1	35	1	0
10	6.73	0	0	8	13.886	0	0	1	37	1	0
11	5.65	2	0	8	12.658	0	0	1	33	0	0
12	5.6	1	0	8	13.108	0	0	1	33	1	0
13	6.85	0	0	8	13.558	0	0	1	33	2	0
14	4.17	0	0	9	12.817	0	0	1	38	0	0
15	5.64	0	0	9	12.918	0	0	1	39	2	0
16	6.44	0	0	9	13.368	0	0	1	40	0	0
17	6.93	0	0	9	13.818	0	0	1	41	0	0
18	7.16	0	0	9	14.268	2	0	1	42	0	0
19	6.95	0	0	8	14.336	1	0	1	38	0	0
20	6.78	0	0	8	13.864	0	0	1	36	0	0
21	6.77	0	0	8	13.864	0	0	1	36	0	0
22	6.53	0	0	8	13.45	0	0	1	33	1	0
23	4.95	0	0	13	13.855	0	0	1	38	1	0
24	6.66	0	0	10	11.22	0	0	2	39	0	4
25	6.60	0	0	8	14.314	0	0	1	36	0	0
26	6.65	0	0	8	14.314	0	0	1	36	0	0

27	7.73	0	0	8	12.64	0	0	0	37	2	0
28	6.6	0	0	8	13.039	0	0	1	36	2	0
29	7.03	0	0	8	13.648	0	0	1	33	0	0
30	6.17	0	0	9	14.194	0	0	1	42	0	0
31	5.44	0	0	9	15.2	0	0	1	44	0	0
32	7.88	0	1	9	12.805	0	0	0	40	0	0
33	7.25	0	0	8	13.652	0	0	1	37	0	0
34	7.61	0	0	8	14.552	2	0	1	39	0	0
35	6.49	0	1	9	12.536	0	1	1	40	0	0
36	6.52	1	1	9	12.536	0	0	1	40	0	0
37	7.62	0	1	9	13.917	0	0	1	41	0	0
38	7.31	0	1	9	13.97	0	0	1	41	0	0
39	6.62	0	0	8	13.204	0	1	0	40	0	0
40	8.02	0	1	9	12.571	0	0	0	40	1	0
41	8.11	0	1	9	13.054	0	0	1	39	0	0
42	7.23	0	0	8	12.644	0	0	0	41	0	1
44	7.23	0	1	9	12.986	0	0	1	41	1	0
45	7.07	1	1	9	12.752	0	0	1	41	0	0
46	5.5	1	0	8	12.839	0	0	2	38	1	1
47	6.21	0	0	9	13.781	0	0	1	41	0	0
48	8.12	0	1	9	12.521	0	0	1	38	0	0
49	7.57	0	1	9	13.202	0	0	1	42	1	0
53	6.38	1	0	8	11.978	0	0	0	39	1	0
54	6.63	0	0	8	13.842	0	0	1	35	1	0
55	7.27	0	0	8	12.428	0	0	1	40	1	0
56	6.91	0	0	8	12.855	0	0	0	36	0	0

Table S4: Correlation matrix between the physicochemical descriptors and alignment independent descriptor influencing the pKa

	pKa	T_N_O_3	HDC	T_2_C_0	XlogP	T_N_O_7	T_N_N_3	T_O_O_2	RBC	T_N_O_4	T_O_O_4	Score
pKa	1	-0.5955	0.4933	-0.2328	-	0.1298	-0.0164	-0.4044	0.1678	-0.0481	-0.0145	11
T_N_O_3	-0.5955	1	-	-0.1068	0.1017	-0.0987	-0.1043	0.1243	-	-0.1005	-0.0309	11
HDC	0.4933	-0.1079	0.1079	0.2541	-	-0.1151	0.1673	-0.1305	0.2742	-0.2589	-0.1217	11
T_2_C_0	-0.2328	-0.1068	1	1	0.3233	0.0279	-0.0136	0.1707	0.4002	-0.1516	0.2024	11
XlogP	-0.1017	-0.3233	0.2541	-0.0148	-	0.2953	-0.1232	0.1569	0.3766	-0.1064	-0.4738	11
T_N_O_7	0.1298	-0.0987	-	0.0279	0.1960	1	-0.0525	0.0626	0.0540	-0.1904	-0.0525	11
T_N_N_3	-0.0164	-0.1043	0.1960	-0.0136	-	-0.0525	1	-0.1853	0.2186	-0.2013	-0.0555	11
T_O_O_2	-0.4044	0.1243	-	0.1707	0.0148	0.0626	-0.1853	1	0.1715	-0.0771	0.4015	11
RBC	0.1678	-0.2742	0.1151	0.3766	1	0.2186	0.1715	-0.2043	-	-0.4195	0.0971	11
T_N_O_4	-0.0481	-0.1005	0.1673	-0.1516	0.2953	-0.1904	-0.2013	-0.0771	0.2043	1	-0.1458	11
T_O_O_4	-0.0145	-0.0309	-	0.2024	-	-0.0525	-0.0555	0.4015	1	-0.1458	1	11
			0.1305		0.1232				-			
			0.4002		0.1569				0.4195			
			-		0.0540				0.0971			
			0.2589		-							
			-		0.1064							
			0.1217		-							
					0.4738							

Table S5: Comparative data of experimental and predicted pKa of heterolipids

Molecules	Experimental pKa	Predicted pKa	Residual
1	6.68	6.684254	-0.004236
3	5.94	5.832331	0.107673
4	6.65	6.684254	-0.034235
6	6.42	6.608259	-0.188249
7	6.43	6.608259	-0.178249
8	7.29	6.693	0.596998
9	6.98	6.693	0.286998
10	6.73	6.593501	0.136511
11	5.65	5.273551	0.376419
12	5.6	6.021107	-0.421123
13	6.85	6.768663	0.081335
14	4.17	4.52068	-0.350687
15	5.64	6.105802	-0.465763
16	6.44	6.29491	0.145116
17	6.93	6.13303	0.796996
18	7.16	7.088005	0.072044
19	6.95	7.165543	-0.215525
20	6.78	6.844558	-0.064557
21	6.77	6.844558	-0.074558
22	6.53	6.965937	-0.435944
23	4.95	4.702767	0.247224
24	6.66	6.549115	0.111069
25	6.6	6.753806	-0.153811
26	6.65	6.753806	-0.10381
27	7.73	7.210132	0.519938
28	6.6	6.659951	-0.059927
29	7.03	7.101499	-0.071514
30	6.17	5.986075	0.183953

31	5.44	5.640939	-0.200912
32	7.88	8.139632	-0.259609
33	7.25	6.816186	0.433823
34	7.61	7.609282	0.00075
35	6.49	6.755043	-0.265102
36	6.52	6.63924	-0.119262
37	7.62	7.303406	0.316574
38	7.31	7.292717	0.017261
39	6.62	6.335997	0.284021
40	8.02	8.01133	0.008701
41	8.11	7.619702	0.490276
42	7.23	7.43973	-0.209655
44	7.21	7.315669	-0.105671
45	7.07	6.524552	0.545429
46	5.5	5.342808	0.15717
47	6.21	6.140492	0.069535
48	8.12	7.79832	0.321657
49	7.57	7.200981	0.36902
53	6.38	6.363077	0.016993
54	6.63	6.744628	-0.114627
55	7.27	7.214597	0.055083
56	6.91	7.048046	-0.138033

Synthesis of Heterolipids

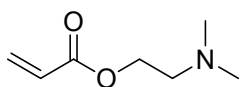
Scheme 1: Synthesis of Series-I bicephalous single tail heterolipids

Synthesis of series I heterolipids involve three simple steps (**Scheme 4.1**), step I involves synthesis of amino acrylates by simple coupling reaction between dimethylamino alcohols and acryloyl chloride, step II involve synthesis of heterodendrons by Michael addition of corresponding amino acrylates with amino alcohols whereas step III consist of Steglich esterification for synthesis of heterolipids with the help of EDAC and DMAP, all the reactions were monitored on TLC plates.

A) Synthesis of amino acrylates (Scheme 1, step I)

a) Synthesis of 2-(dimethylamino) ethyl acrylate, 3a

To a cooled (0 °C) solution of 2-Dimethylaminoethanol 2a (5 g, 56.09 mmol) in a mixture of 100 mL of tetrahydrofuran (THF) and triethylamine (ETN) (23.43 mL, 168.27 mmol), was added drop wise acryloyl chloride 1 (6.09 g, 67.3 mmol) under nitrogen and the reaction mixture was stirred for 3 h. After the completion of the reaction, the reaction mixture was filtered and product was purified by column chromatography using neutral alumina and dichloromethane (DCM) as mobile phase to offer 2-(dimethylamino) ethyl acrylate 3a as slightly yellow liquid (7.42 g, 92.38 %).



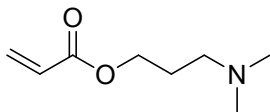
2-(dimethylamino)ethyl acrylate

FT-IR (neat) v: 2949, 2771, 1726, 1631, 1460, 1408, 1273, 1188, 1053 cm⁻¹.

¹H NMR (CDCl₃) δ: 2.26 (s, 6H), 2.56 (t, 2H), 4.25 (t, 2H), 5.89 (dd, 1H), 6.17 (dd, 1H), 6.45 (dd, 1H)

b) Synthesis of 3-(dimethylamino) propyl acrylate 3b

3-Dimethylamino-1-propanol 2b (5 g, 48.4 mmol) dissolved in 100 mL tetrahydrofuran (THF) with triethylamine (ETN) (20.24 mL, 145.2 mmol), followed by drop wise addition of acryloyl chloride 1 (5.26 g, 58.1 mmol) under nitrogen and reaction mixture stirred at 0 °C for 3 h. After reaction completion mixture was filtered and product was purified by column chromatography using neutral alumina and dichloromethane (DCM) as mobile phase offered as 3-(dimethylamino) propyl acrylate 3b as slightly yellow liquid (6.88 g, 90.29 %).



3-(dimethylamino)propyl acrylate

FT-IR (neat) v: 2949, 2818, 1726, 1633, 1462, 1408, 1271, 1195, 1058 cm^{-1}

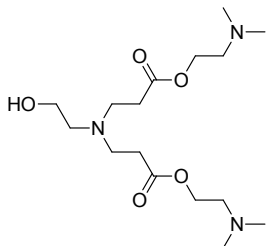
$^1\text{H NMR (CDCl}_3)$ δ : 1.88 (p/m, 2H), 2.29 (s, 6H), 2.41 (t, 2H), 4.22 (t, 2H), 5.84 (dd, 1H), 6.19 (dd, 1H), 6.44 (dd, 1H)

B] Synthesis of heterodendrons 5a-5d (HD-22, HD-32, HD-23, and HD-33) (Scheme 1, step-II)

a) bis(2-(dimethylamino)ethyl)3,3'-((2-hydroxyethyl)azanediyl)dipropanoate 5a (HD-22)

Michael addition between ethanolamine 4a (0.5 g, 8.15 mmol) and 2-(Dimethyl amino) ethyl acrylate 3a (4.687 g, 32.74 mmol) was carried out; ethanolamine was added dropwise to 2-(Dimethyl amino) ethyl acrylate at 0 °C. After complete of addition reaction temperature rose to room temperature (RT) and stirred for 48 h, allowed to stand for overnight and evaporated in vacuo to obtain pure bis(2-(dimethylamino)ethyl) 3,3'-((2-hydroxyethyl)azanediyl)dipropanoate 5a (HD-22) as slightly yellow liquid (2.69 g, 94.57 %).

a) bis(2-(dimethylamino)ethyl) 3,3'-((2-hydroxyethyl)azanediyl)dipropanoate 5a (HD-22)



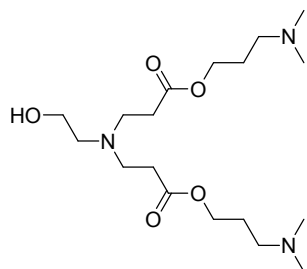
bis(2-(dimethylamino)ethyl) 3,3'-((2-hydroxyethyl)azanediyl)dipropanoate

FT-IR (neat) v: 3307, 2943, 2827, 1732, 1460, 1265, 1176, 1045 cm^{-1}

$^1\text{H NMR (CDCl}_3)$ δ : 1.18 (s, 1H), 2.29 (s, 12H), 2.41 (t, 4H), 2.50 (t, 4H), 2.72 (t, 4H), 3.41 (t, 2H), 3.60 (t, 2H), 4.11 (t, 4H)

b) bis(3-(dimethylamino)propyl)3,3'-((2-hydroxyethyl)azanediyl)dipropanoate 5b (HD-32)

Michael addition between 3-amino-1-propanol 4b (0.5 g, 6.65 mmol) and 2-(Dimethyl amino) ethyl acrylate 3a (3.81 g, 26.62 mmol), 3-amino-1-propanol was added dropwise to 2-(Dimethyl amino) ethyl acrylate at 0 °C. After complete of addition reaction temperature rose to RT and stirred for 48 h, allowed to stand for overnight and evaporated in vacuo to obtain pure bis(3-(dimethylamino)propyl) 3,3'-((2-hydroxyethyl)azanediyl)dipropanoate 5b (HD-32) as slightly yellow liquid (2.32 g, 93.31 %).



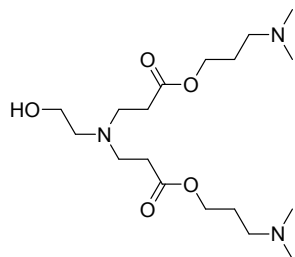
bis(3-(dimethylamino)propyl) 3,3'-((2-hydroxyethyl)azanediyl)dipropanoate

FT-IR (neat) v: 3352, 2945, 2827, 1735, 1462, 1271, 1174, 1039 cm^{-1}

$^1\text{H NMR (CDCl}_3)$ δ : 1.19 (m 2H), (s, 1H of OH), 2.23 (s, 12H), 2.42 (t, 4H), 2.54 (t, 4H), 2.73 (t, 4H), 3.64 (t, 2H), 4.01 (t, 2H), 4.12 (t, 4H)

c) bis(2-(dimethylamino)ethyl)3,3'-((3-hydroxypropyl)azanediyl)dipropanoate 5c (HD-23)

Michael addition between ethanolamine 4a (0.5 g, 8.15 mmol) and 3-(Dimethyl amino) propyl acrylate 3b (5.14 g, 32.74 mmol), ethanolamine was added dropwise to 3-(Dimethyl amino) propyl acrylate at 0 °C. After complete of addition reaction temperature rose to RT and stirred for 48 h, allowed to stand for overnight and evaporated in vacuo to obtain pure bis(2-(dimethylamino)ethyl) 3,3'-((3-hydroxypropyl)azanediyl)dipropanoate 5c (HD-23) as slightly yellow liquid (2.76 g, 93.27 %).



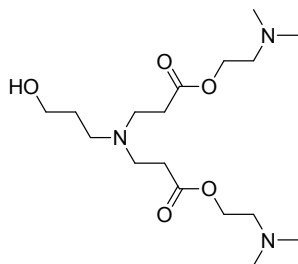
bis(2-(dimethylamino)ethyl) 3,3'-((3-hydroxypropyl)azanediyl)dipropanoate

FT-IR (neat) v: 3304, 2943, 2827, 1732, 1460, 1267, 1174, 1043 cm^{-1}

¹H NMR (CDCl₃) δ: 1.75 (m, 4H), 2.19 (s, 12H), 2.31 (t, 4H), 2.42 (t, 4H), 2.53 (m, 4H), 3.54 (t, 2H), 3.66 (s, 1H), 3.75 (t, 2H), 4.08 (t, 4H).

d) bis(3-(dimethylamino)propyl)3,3'-((3-hydroxypropyl)azanediyl)dipropoate, 5d HD-33)

Michael addition between 3-amino-1-propanol 4b ((0.5 g, 6.65 mmol)) and 3-(Dimethyl amino) propyl acrylate 3b (4.186g, 26.62 mmol), 3-amino-1-propanol was added dropwise to 3-(Dimethyl amino) propyl acrylate at 0 °C. After complete of addition reaction temperature rose to RT and stirred for 48 h, allowed to stand for overnight and evaporated in vacuo to obtain pure bis(3-(dimethylamino)propyl) 3,3'-((3-hydroxypropyl)azanediyl)dipropoate 5d (HD-33) as slightly yellow liquid (2.46 g, 95.36 %).



bis(2-(dimethylamino)ethyl) 3,3'-((3-hydroxypropyl)azanediyl)dipropoate

FT-IR (neat) v: 3360, 2945, 2823, 1732, 1465, 1257, 1176, 1043 cm⁻¹

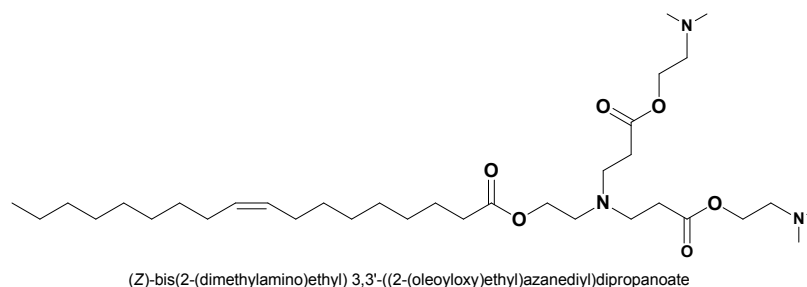
¹H NMR (CDCl₃) δ: 1.64 (p/m, 2H), 1.78 (p/m, 4H), 2.20 (s, 12H), 2.32 (t, 4H), 2.46 (t, 4H), 2.58 (t, 2H), 2.76 (t, 4H), 3.45 (s, 1H), 3.68 (t, 2H), 4.10 (t, 4H).

C] Synthesis of Heterolipids 7a-7d (HL-22, HL-32, HL-23 and HL-33) (Scheme 1, step-III)

a) (Z)-bis(2-(dimethylamino)ethyl)3,3'-((2-(oleoyloxy)ethyl)azanediyl)dipropoate, 7a (HL-22)

Oleic acid 6 (1 g, 3.54 mmol) with bis(2-(dimethylamino)ethyl) 3,3'-((2-hydroxyethyl)azanediyl)dipropoate 5a (1.23, 3.54 mmol) dissolved in 50 mL of DCM in presence of EDAC (0.678 g, 3.54 mmol) and catalytical amount of DMAP. Addition of all chemicals were carryout at 10 °C after complete addition reaction temperature rose to RT slowly and stirred for 16 hr. Solvent from reaction mixture was removed under reduced pressure and residue obtained was purified by column chromatography (SiO₂) using DCM/MeOH, 10:2 as eluent to afford (Z)-bis(2-(dimethylamino)ethyl) 3,3'-((2-

(oleoyloxy)ethyl)azanediyl)dipropoanoate 7a (HL-22) as colorless to slightly yellow liquid (1.95 g, 90.01 %).



FT-IR (neat) v: 2926, 1737, 1622, 1462, 1201, 1080 cm^{-1}

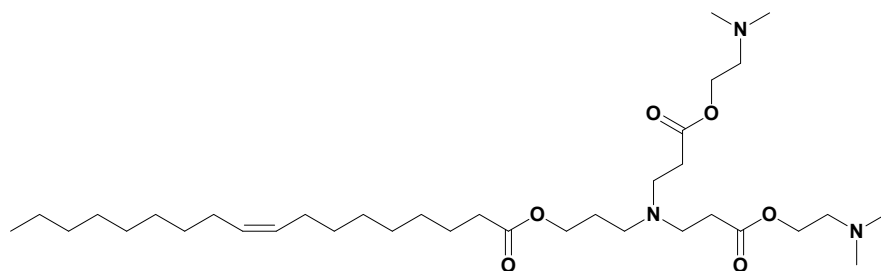
^1H NMR (CDCl₃) δ : 0.86 (t, 3H), 1.26 (m, 20H), 1.60 (m, 2H), 1.82(t, 2H), 2.00(t, 4H), 2.28(s, 12H) 2.47(t, 4H) 2.57(t, 4H) 2.70 (t, 2H), 2.83 (t, 4H) 4.10 (t, 2H) 4.17 (t, 4H) 5.34 (q/m 2H),

^{13}C NMR (CDCl₃) δ : 14.05, 22.64, 27.16, 29.10, 29.17, 29.29, 29.49, 29.69, 31.87, 32.81, 45.39, 49.75, 52.10, 57.55, 60.33, 61.92, 129.72, 129.97, 172.27, 173.64.

ESI-HRMS m/z: 612.19 [M⁺]

b) (Z)-bis(2-(dimethylamino)ethyl)3,3'-((3-oleoyloxy)propyl)azanediyl)dipropoanoate 7b (HL-32)

Oleic acid 6 (1 g, 3.54 mmol) with bis(3-(dimethylamino)propyl) 3,3'-((2-hydroxyethyl)azanediyl)dipropoanoate 5b (1.279 g, 3.54 mmol) dissolved in 50 mL of DCM in presence of EDAC (0.678 g, 3.54 mmol) and catalytical amount of DMAP. Addition of all chemicals was carryout at 10 °C after complete addition reaction temperature rose to RT slowly and stirred for 16 hr. Solvent from reaction mixture was removed under reduced pressure and residue obtained was purified by column chromatography (SiO₂) using DCM/MeOH, 10:2 as eluent to afford (Z)-bis(2-(dimethylamino)ethyl) 3,3'-((3-(oleoyloxy)propyl)azanediyl)dipropoanoate 7b (HL-32) as colorless to slightly yellow liquid (2.06 g, 2.96 %).



(Z)-bis(2-(dimethylamino)ethyl) 3,3'-((3-(oleoyloxy)propyl)azanediyl)dipropionate

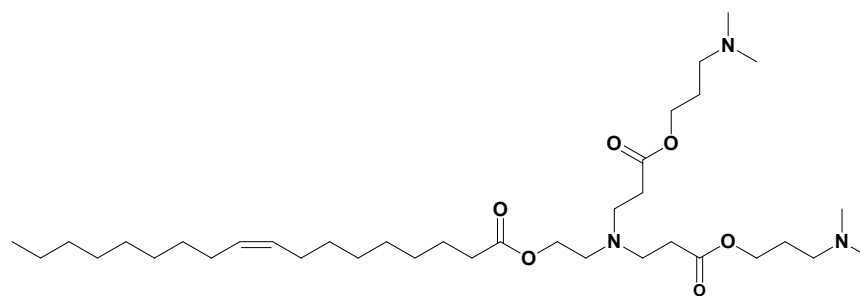
FT-IR (neat) v: 2924, 2854, 1735, 1462, 1218, 1193, 1085 cm^{-1}

^1H NMR (CDCl_3) δ : 0.90 (t, 3H), 1.29 (m, 20H), 1.78 (m, 2H), 2.02 (m, 2H), 2.34(t, 4H), 2.45(t, 2H), 2.47(s, 12H) 2.50 (t, 4H) 2.52 (t 2H), 2.63(t, 4H), 2.78 (t, 4H) 4.08 (t, 2H) 4.21 (t, 4H) 5.37 (q/m 2H),

^{13}C NMR (CDCl_3) δ : 14.06, 22.64, 24.97, 27.20, 29.11, 29.17, 29.28, 29.30, 29.49, 29.69, 29.74, 31.87, 32.57, 45.43, 49.18, 52.19, 57.58, 61.95, 62.33, 129.73, 129.97, 172.45, 173.76. **ESI-HRMS m/z:** 626.51 [M+]

c) (Z)-bis(3-(dimethylamino)propyl)3,3'-((2-(oleoyloxy)ethyl)azanediyl)dipropionate 7c (HL-23)

Oleic acid **6** (1 g, 3.54 mmol) with bis(2-(dimethylamino)ethyl) 3,3'-((3-hydroxypropyl)azanediyl)dipropionate **5c** (1.32 g, 3.54 mmol) dissolved in 50 mL of DCM in presence of EDAC (0.678 g, 3.54 mmol) and catalytical amount of DMAP. Addition of all chemicals was carryout at 10 °C after complete addition reaction temperature rose to RT slowly and stirred for 16 hr. Solvent from reaction mixture was removed under reduced pressure and residue obtained was purified by column chromatography (SiO_2) using DCM/MeOH, 10:2 as eluent to afford (Z)-bis(3-(dimethylamino)propyl) 3,3'-((2-(oleoyloxy)ethyl)azanediyl)dipropionate **7c** (HL-23) as colorless to slightly yellow liquid (2.04 g, 90.04 %).



(Z)-bis(3-(dimethylamino)propyl) 3,3'-((2-(oleoyloxy)ethyl)azanediyl)dipropionate

FT-IR (neat) v: 2924, 2852, 1735, 1462, 1217, 1083 cm^{-1}

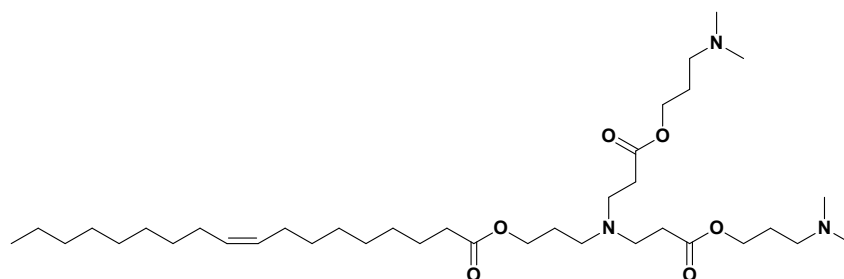
^1H NMR (CDCl₃) δ : 0.90 (t, 3H), 1.29 (m, 20H), 2.02 (m, 4H), 2.29 (m, 2H), 2.31(t, 4H), 2.46(t, 2H), 2.48(s, 12H) 2.50 (t, 4H) 2.52 (t 4H), 2.61(t, 2H), 2.78 (t, 4H) 4.08 (t, 2H) 4.19 (t, 4H) 5.36 (q/m 2H),

^{13}C NMR (CDCl₃) δ : 14.07, 22.64, 27.17, 29.09, 29.16, 29.27, 29.48, 29.72, 31.86, 45.36, 49.66, 52.00, 57.49, 60.34 61.86, 62.16, 129.69, 129.93, 172.27, 173.63.

ESI-HRMS m/z: 640.52 [M⁺]

d) (Z)-bis(3-(dimethylamino)propyl)3,3'-((3-(oleoyloxy)propyl)azanediyl)dipropionate, 7d (HL-33)

HL-33 was synthesized by coupling of oleic acid 6 (1 g, 3.54 mmol) with bis(3-(dimethylamino)propyl) 3,3'-((3-hydroxypropyl)azanediyl)dipropionate 5d (1.37 g, 3.54 mmol) dissolved in 50 mL of DCM in presence of EDAC (0.678 g, 3.54 mmol) and catalytical amount of DMAP. Addition of all chemicals was carryout at 10 °C after complete addition reaction temperature rose to RT slowly and stirred for 16 hr. Solvent from reaction mixture was removed under reduced pressure and residue obtained was purified by column chromatography (SiO₂) using DCM/MeOH 10:2 as eluent to afford (Z)-bis(3-(dimethylamino)propyl) 3,3'-((3-(oleoyloxy)propyl)azanediyl)dipropionate7d (HL-33) as colorless to slightly yellow liquid (2.16 g, 93.29 %).



(Z)-bis(3-(dimethylamino)propyl) 3,3'-((3-(oleoyloxy)propyl)azanediyl)dipropionate

FT-IR (neat) v: 2926, 2856, 1735, 1456, 1251, 1182, 1047 cm^{-1}

^1H NMR (CDCl_3) δ : 0.88 (t, 3H), 1.28 (m, 20H), 1.71 (m, 4H), 2.02 (m, 2H), 2.03 (m, 2H), 2.18(m, 4H), 2.19(s, 12H), 2.36 (t, 4H), 2.38 (t, 4H) 2.50 (t 4H), 2.60(t, 2H), 3.50 (t, 4H) 3.61 (t, 2H) 4.19 (t, 2H) 5.34 (q/m 2H),

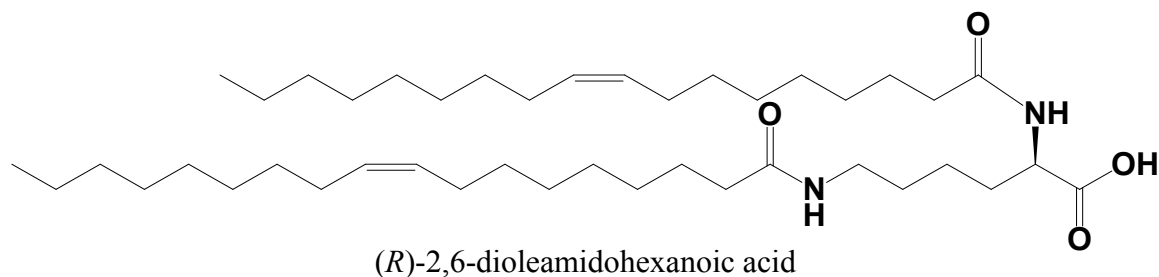
^{13}C NMR (CDCl_3) δ : 14.11, 22.67, 27.21, 29.31, 29.39, 29.45, 29.52, 29.76, 31.90, 41.44, 43.30, 45.32, 56.03, 58.09, 61.30, 63.37, 129.75, 130.00, 170.89, 174.65.

ESI-HRMS m/z: 654.54 [M⁺]

Scheme II: Synthesis of series-II lysine based monocephalous two tail heterolipids.

A) Synthesis of (R)-2, 6-dioleamidohexanoic acid 10 (Scheme 2, Step I)

(R)-2,6-diaminohexanoic acid 9 (2g, 9.12 mmol) was added in 100 mL aq. NaOH solution (pH 8) followed by addition of THF after that dropwise addition of oleoyl chloride 8 (5.49 g, 18.25 mmol) was carried out at 10 °C, during oleoyl chloride addition pH of reaction was monitored and kept around pH 8 by adding small aliquots of dilute NaOH . After complete addition reaction temperature rose to room temperature and stirred for 3h. After reaction completion dilute HCl was added to make reaction mixture neutral pH, both organic and aqueous layers were separated and product from organic layer was purified by column chromatography (SiO_2) using DCM/MeOH, 10:1 as eluent to afford (R)-2, 6-dioleamidohexanoic acid 10 as white semisolid (6.58 g, 89.01 %).



FT-IR (neat) v: 3300, 2926, 2856, 1643, 1550, 1456, 1193, 1070 cm^{-1}

^1H NMR (CDCl_3) δ : 0.89 (t, 6H), 1.51 (m, 42H), 1.62 (m, 2H), 1.85 (t, 4H), 1.90 (m, 2H), 2.03 (t, 8 H), 2.20 (m, 4H), 3.29 (m, 2H), 4.56 (t, 1H), 5.37 (m, 4H), 6.071 (t, 1H), 6.78 (d, 1H), 7.91 (s, 1H)

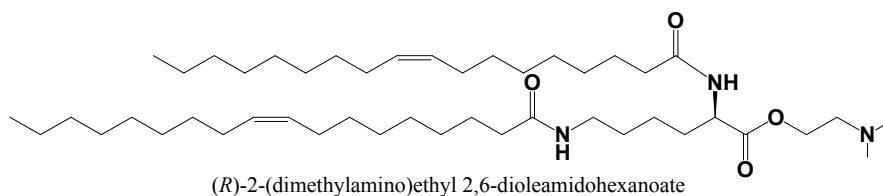
^{13}C NMR (CDCl_3) δ : 14.15, 22.05, 22.71, 25.72, 25.84, 27.25, 28.99, 29.21, 29.23, 29.35, 29.56, 29.72, 29.79, 31.35, 31.93, 36.45, 36.76, 38.82, 52.06, 129.70, 129.72, 130.02, 130.25, 174.27, 174.36, 174.50.

ESI-MS m/z: 675.12 [M⁺].

B] Synthesis of lysine based heterolipids (HLys E2, HLys E3, HLys A2 and HLys A3) (Scheme 2, Step II)

a) Synthesis of (*R*)-2-(dimethylamino)ethyl 2,6-dioleamidohexanoate 12a (HLys E2)

2-Dimethylaminoethanol 2a (0.132g, 1.48 mmol) with (*R*)-2,6-dioleamidohexanoic acid 10 (1 g, 1.48 mmol) dissolved in 50 mL of DCM in presence of EDAC (0.283 g, 1.48 mmol) and catalytical amount of DMAP. Addition of all chemicals was carryout at 10 °C after complete addition reaction temperature rose to RT slowly and stirred for 16 hr. Solvent from reaction mixture was removed under reduced pressure and residue obtained was purified by column chromatography (SiO_2) using DCM/MeOH 10:1 as eluent to afford (*R*)-2-(dimethylamino)ethyl 2,6-dioleamidohexanoate 12a as colorless to slightly yellow oily liquid (1.02 g, 92.27 %).



FT-IR (neat) v: 2925, 2853, 1741, 1644, 1549, 1463, 1176, 1099 cm^{-1}

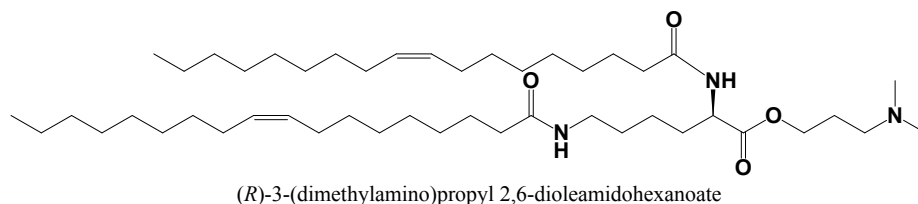
$^1\text{H NMR (CDCl}_3)$ δ : 0.90 (t, 6H), 1.29 (m, 42H), 1.55 (m, 2H), 1.66 (t, 4H), 1.85 (m, 2H), 2.04 (t, 8 H), 2.23 (m, 4H), 2.40, (s, 6H), 2.57, (t, 2H), 3.27 (m, 2H), 4.24, (t, 2H), 4.55 (m, 1H) 5.37 (m, 4H), 5.73 (t 1H), 6.25(d, 1H),

$^{13}\text{C NMR (CDCl}_3)$ δ : 14.10, 22.67, 27.18, 27.21, 29.28, 29.30, 29.51, 29.76, 31.89, 45.30, 51.75, 55.95, 129.72, 129.98, 172.61, 173.22, 173.44,

ESI-HRMS m/z: 746.67 [M⁺].

b) Synthesis of (R)-3-(dimethylamino)propyl 2,6-dioleamido hexanoate 12b (HLys E3)

3-Dimethylamino-1-propanol 2b (0.152g, 1.48 mmol) (R)-2,6-dioleamido hexanoic acid 10 (1 g, 1.48 mmol) dissolved in 50 mL of DCM in presence of EDAC (0.283 g, 1.48 mmol) and catalytical amount of DMAP. Addition of all chemicals was carryout at 10 °C after complete addition reaction temperature rose to RT slowly and stirred for 16 hr. Solvent from reaction mixture was removed under reduced pressure and residue obtained was purified by column chromatography (SiO₂) using DCM/MeOH 10:1 as eluent to afford HLys E3 12b as colorless to slightly yellow oily liquid (0.99 g, 88.53 %).



FT-IR (neat) v: 2924, 2854, 1741, 1644, 1549, 1463, 1176, 1099 cm^{-1}

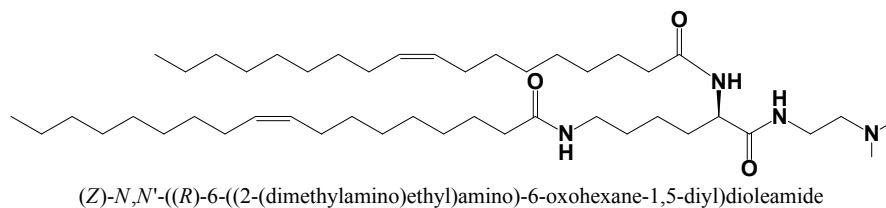
$^1\text{H NMR (CDCl}_3)$ δ : 0.90 (t, 6H), 1.32 (m, 42H), 1.55 (m, 2H), 1.69 (t, 4H), 1.82 (m, 2H), 2.03 (t, 8 H), 2.22 (m, 4H), 2.24, (s, 6H), 2.37, (m, 2H), 3.26 (m, 2H), 4.23, (t, 2H), 4.59 (m, 1H) 5.36 (m, 4H), 5.72 (t 1H), 6.16(d, 1H),

$^{13}\text{C NMR (CDCl}_3)$ δ : 14.11, 22.68, 27.18, 27.22, 29.31, 29.52, 29.73, 29.76, 31.90, 44.98, 51.74, 55.81, 63.46, 129.73, 129.99, 172.59, 172.93, 173.26,

ESI-HRMS m/z: 760.69 [M⁺].

c) Synthesis of (Z)-N,N'-((R)-6-((2-(dimethylamino)ethyl)amino)-6-oxohexane-1,5-diyl)dioleamide 12c (HLys A2)

N,N-dimethylethane-1,2-diamine 11a (0.13 g, 1.48 mmol) with (R)-2,6-dioleamidohexanoic acid 10 (1 g, 1.48 mmol) dissolved in 50 mL of DCM in presence of EDAC (0.283 g, 1.48 mmol) and HOBt (0.195 g, 1.48 mmol). Addition of all chemicals was carryout at 10 °C after complete addition reaction temperature rose to RT slowly and stirred for 16 hr. Solvent from reaction mixture was removed under reduced pressure and residue obtained was purified by column chromatography (SiO₂) using DCM/MeOH 10:1 as eluent to afford HLys A2 12c as colorless sticky solid. (1.06 g, 96.02 %).



FT-IR (neat) v: 2922, 2851, 1642, 1553, 1466, 1382, 1278 cm⁻¹

¹H NMR (CDCl₃) δ: 0.90 (t, 6H), 1.33 (m, 42H), 1.55 (m, 2H), 1.65 (t, 4H), 1.82 (m, 2H), 2.02 (t, 8 H), 2.22 (m, 4H), 2.28, (s, 6H), 2.46, (m, 2H), 3.31 (m, 4H), 4.40 (m, 1H) 5.37 (m, 4H), 5.65 (t 1H), 6.32 (d, 1H), 6.57 (t, 1H),

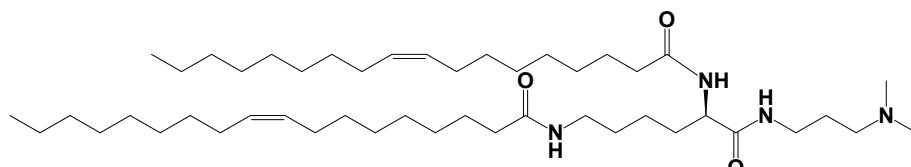
¹³C NMR (CDCl₃) δ: 14.11, 22.67, 27.21, 29.20, 29.24, 29.30, 29.35, 29.52, 29.70, 29.76, 31.89, 43.92, 53.28, 57.64, 129.74, 129.96, 172.92, 173.51, 174.11,

ESI-HRMS m/z: 745.69 [M⁺].

d) Synthesis of (Z)-N,N'-((R)-6-((3-(dimethylamino)propyl)amino)-6-oxohexane-1,5-diyl)dioleamide 12d (HLys A3)

N1,N1-dimethylpropane-1,3-diamine 11b (0.151 g, 1.48 mmol) with (R)-2,6-dioleamidohexanoic acid 10 (1 g, 1.48 mmol) dissolved in 50 mL of DCM in presence of EDAC (0.283 g, 1.48 mmol) and HOBt (0.195 g, 1.48 mmol).. Addition of all chemicals was carryout at 10 °C after complete addition reaction temperature rose to RT slowly and stirred for 16 hr. Solvent from reaction mixture was removed under reduced pressure and residue obtained was purified by column

chromatography (SiO₂) using DCM/MeOH 10:1 as eluent to afford HLys A3 12d as colorless sticky solid (1.01 g, 89.89 %).



(Z)-N,N'-((R)-6-((3-(dimethylamino)propyl)amino)-6-oxohexane-1,5-diyldioleamide

FT-IR (neat) v: 2922, 2851, 1639, 1553, 1466, 1378, 1278, 989 cm⁻¹

¹H NMR (CDCl₃) δ: 0.81 (t, 6H), 1.23 (m, 42H), 1.47 (m, 2H), 1.59 (t, 4H), 1.46 (m, 2H), 1.78 (m, 2H), 1.93 (t, 8 H), 2.09 (m, 4H), 2.19 (m, 2H) 2.41, (s, 6H), 2.62, (m, 2H), 3.18 (m, 2H), 3.31 (m, 2H), 4.24 (m, 1H) 5.27 (m, 4H), 5.67 (t 1H), 6.33 (d, 1H), 7.63 (t, 1H),

¹³C NMR (CDCl₃) δ: 14.11, 22.67, 25.86, 27.20, 27.22, 29.20, 29.21, 29.31, 29.32, 29.52, 29.76, 31.89, 44.09, 53.26, 56.58, 129.73, 129.99, 172.52, 173.69, 173.93,

ESI-HRMS m/z: 759.70 [M⁺].

Figure S1: ¹H NMR spectra of *Z*-bis(2-(dimethylamino)ethyl) 3,3'-((2-(oleoyloxy)ethyl)azanediyl)dipropanoate 7a (HL-22)

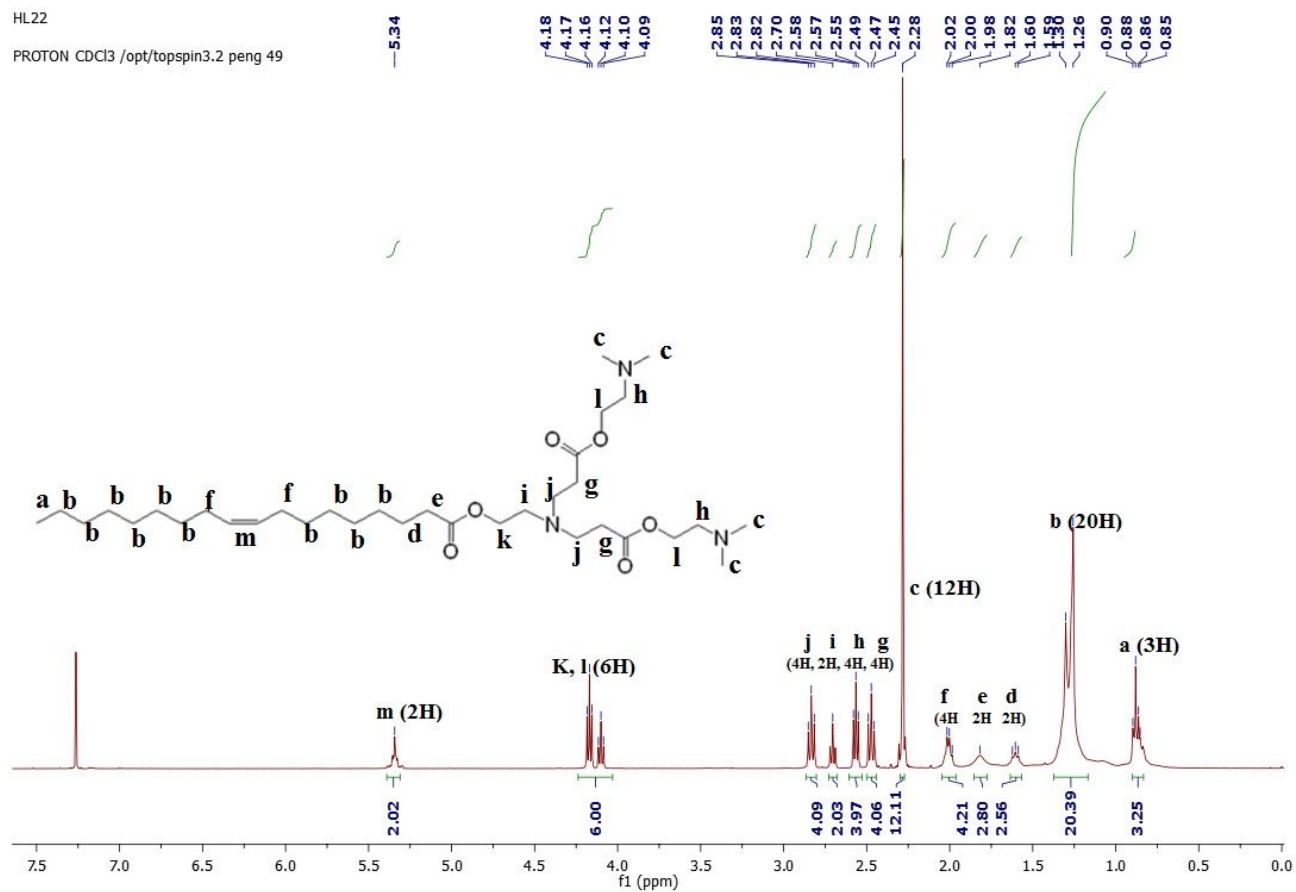


Figure S2: ^{13}C NMR spectra of *Z*-bis(2-(dimethylamino)ethyl) 3,3'-((2-(oleoyloxy)ethyl)azanediyl)dipropanoate 7a (HL-22)

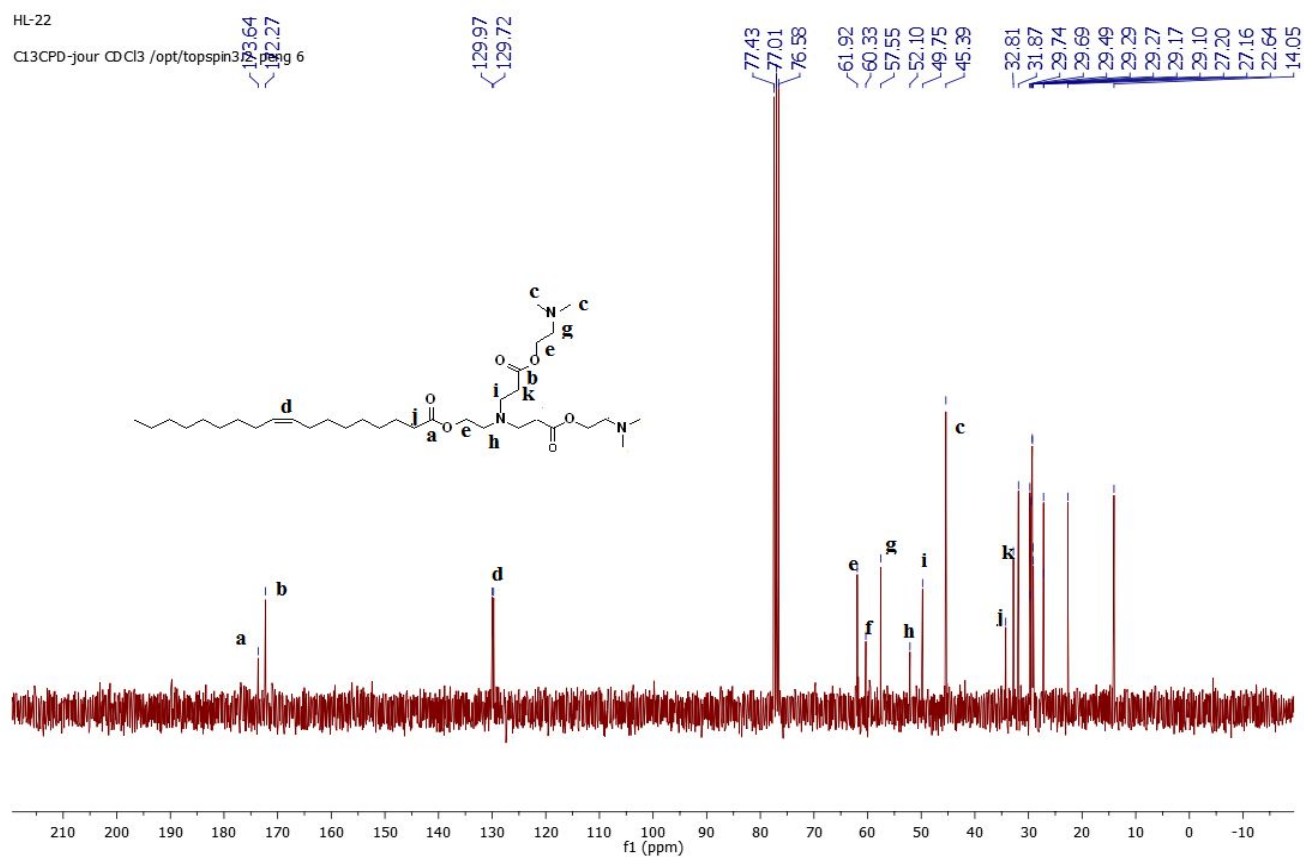
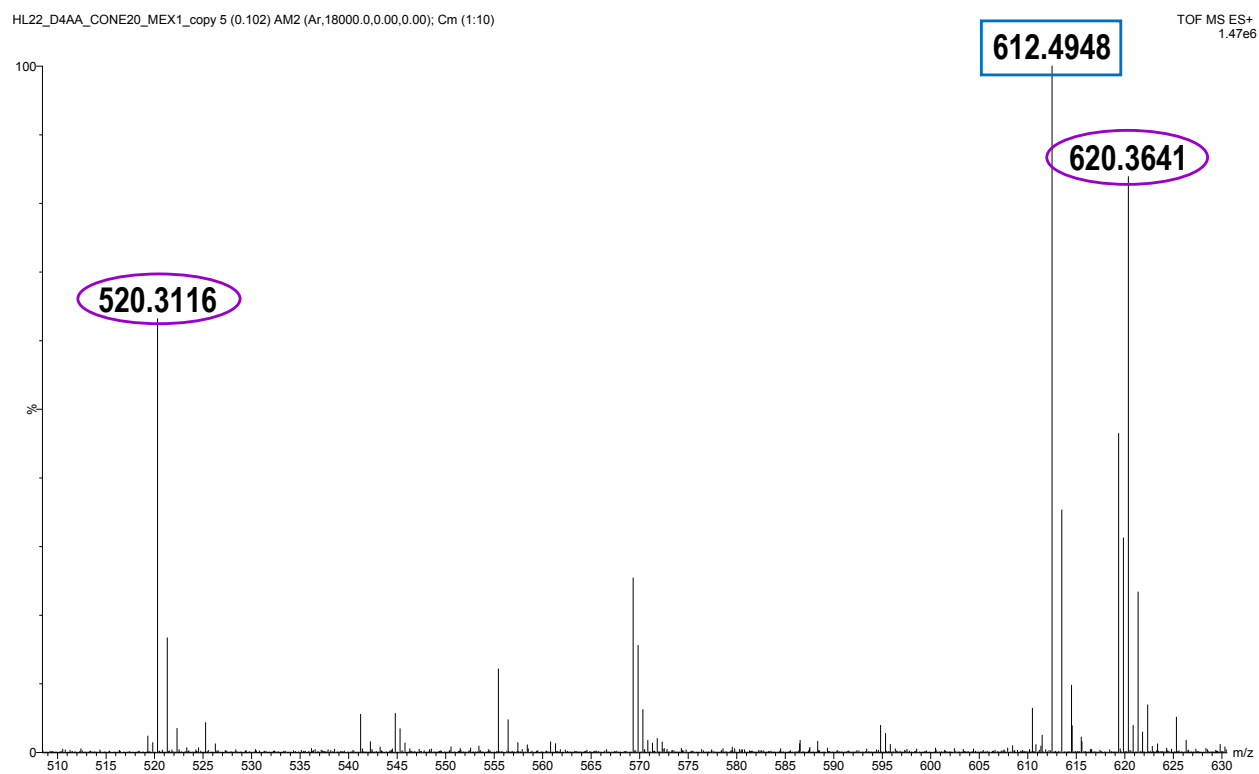


Figure S3: High resolution mass spectrum in electrospray positive mode of (Z)-bis(2-(dimethylamino)ethyl) 3,3'-((2-(oleoyloxy)ethyl)azanediyldipropionate 7a (HL-22)



(The target ion is detected at m/z 612.4948 and the peaks retained for internal calibration are observed at m/z 520.3116 and m/z 620.3641, respectively)

Figure S4: ^1H NMR spectra of (Z)-bis(2-(dimethylamino)ethyl)3,3'-((3(oleoyloxy)propyl)azanediyl)dipropionate 7b (HL-32)

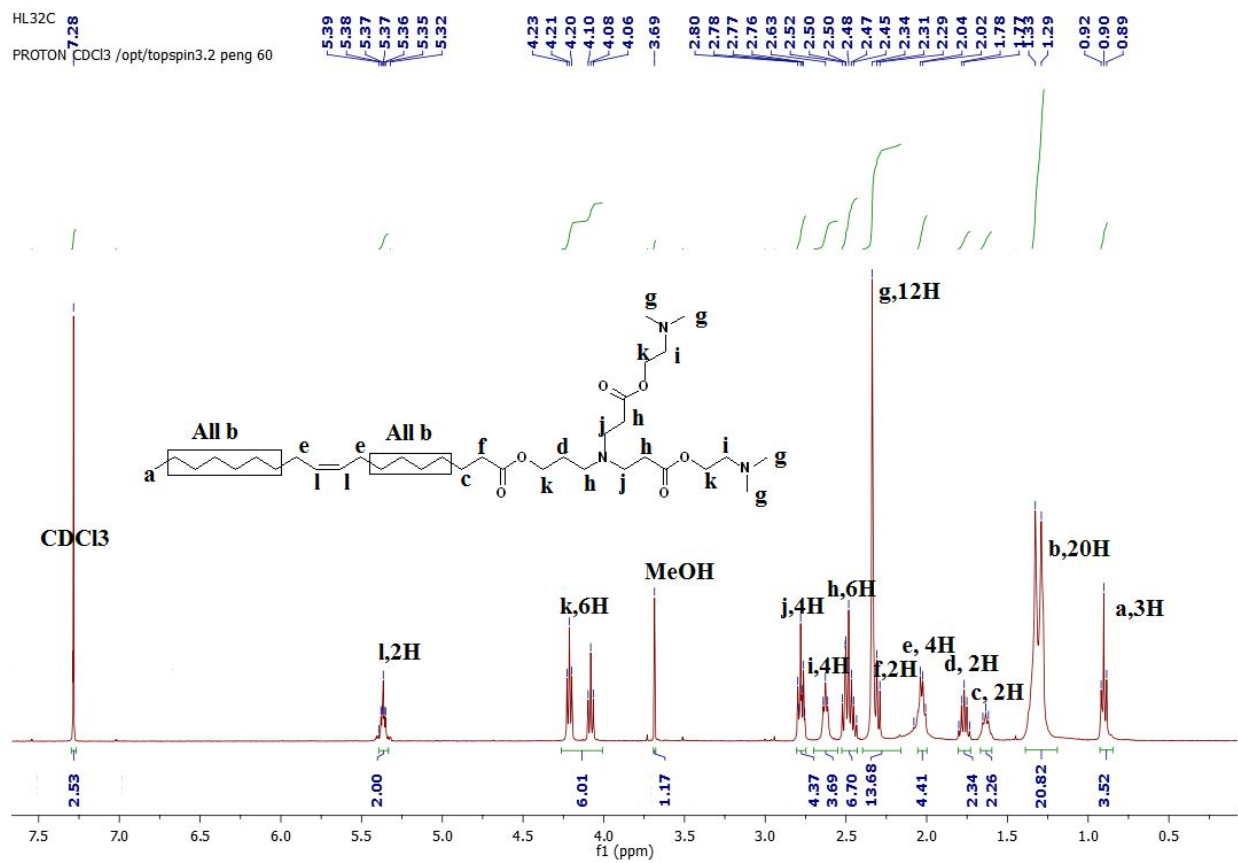


Figure S5: ^{13}C NMR spectra of (Z)-bis(2-(dimethylamino)ethyl)3,3'-((3(oleoyloxy)propyl)azanediyl)dipropionate 7b (HL-32)

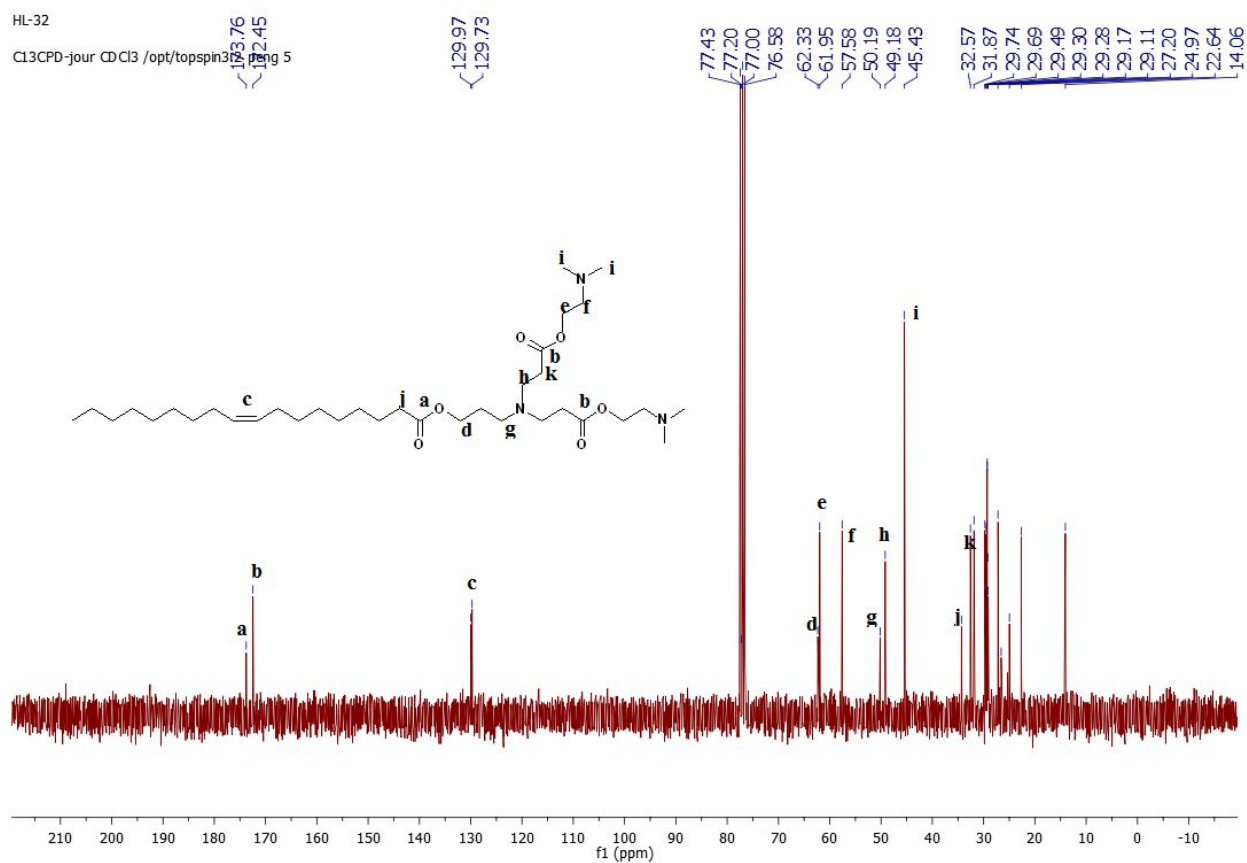
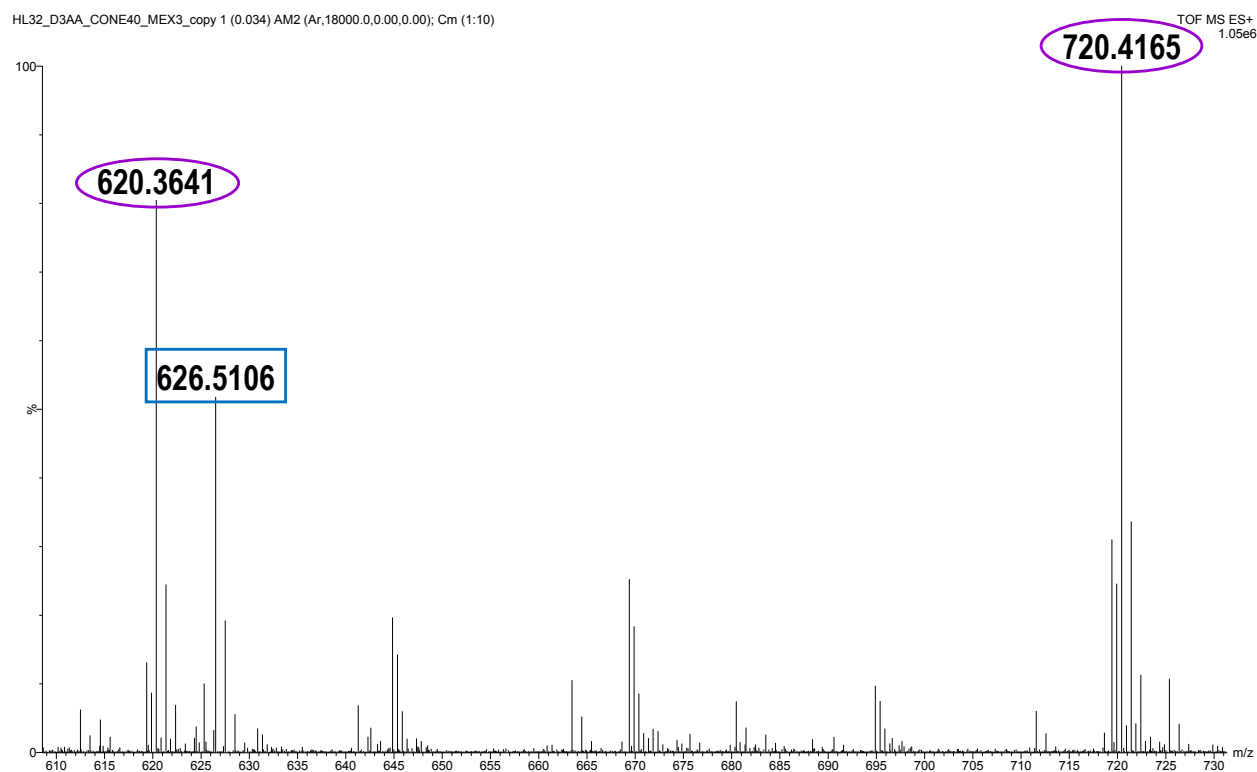


Figure S6: High resolution mass spectrum in electrospray positive mode of the (Z)-bis(2-(dimethylamino)ethyl)3,3'-((3(oleoyloxy)propyl)azanediyl)dipropionate 7b (HL-32)



(The target ion is detected at m/z 626.5106 and the peaks retained for internal calibration are observed at m/z 620.3641 and m/z 720.4165, respectively)

Figure S7: ¹H NMR spectra of (Z)-bis(3-(dimethylamino)propyl)3,3'-((2(oleoyloxy)ethyl)azanediyl)dipropanoate 7c (HL-23)

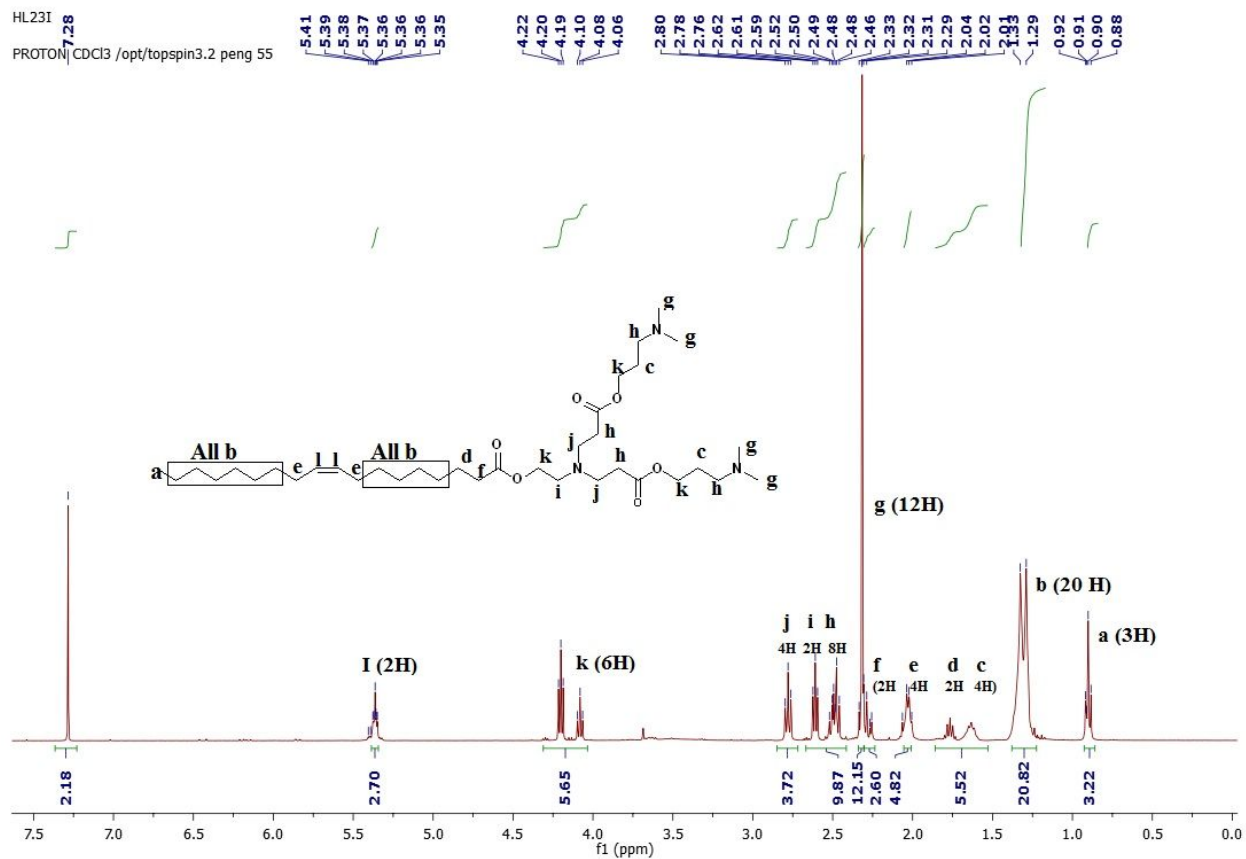


Figure S8: ^{13}C NMR spectra of (Z)-bis(3-(dimethylamino)propyl)3,3'-((2(oleoyloxy)ethyl)azanediyldipropionate 7c (HL-23)

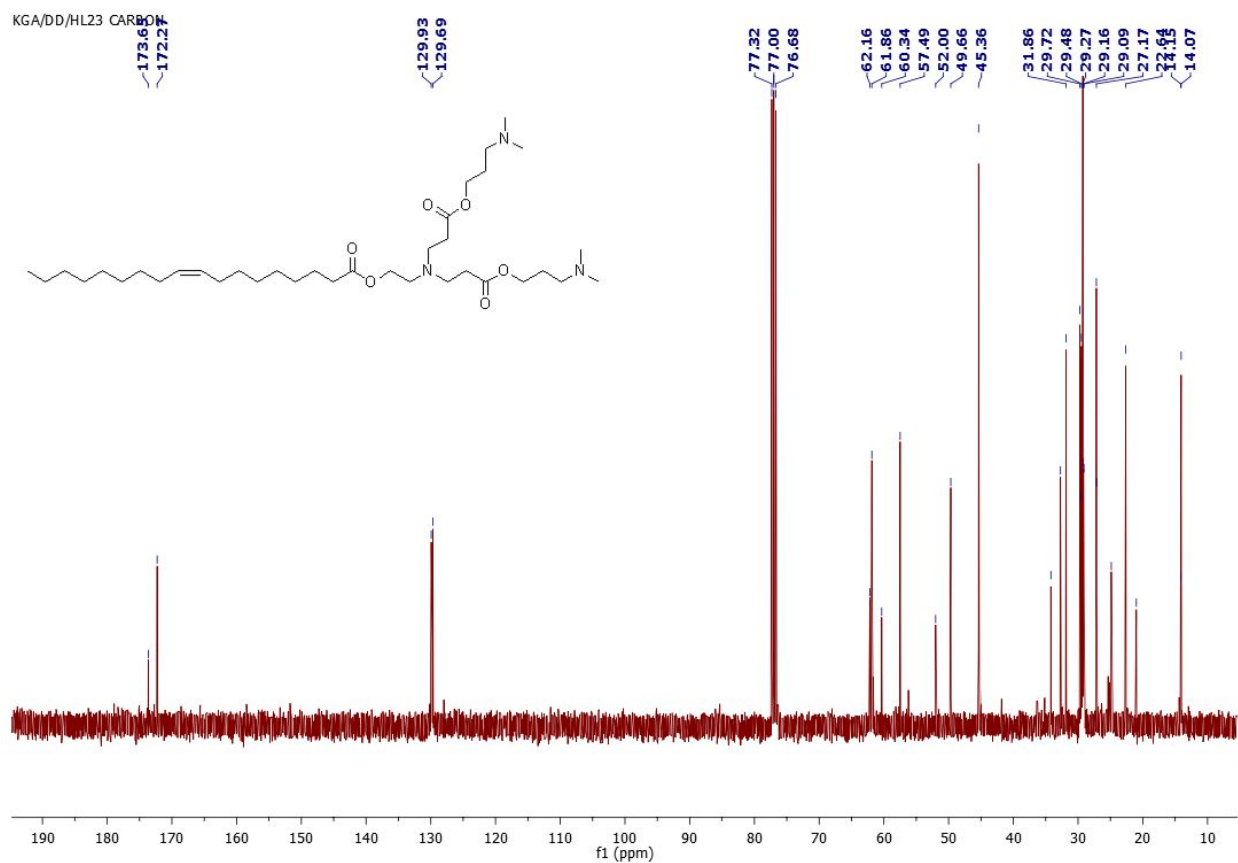
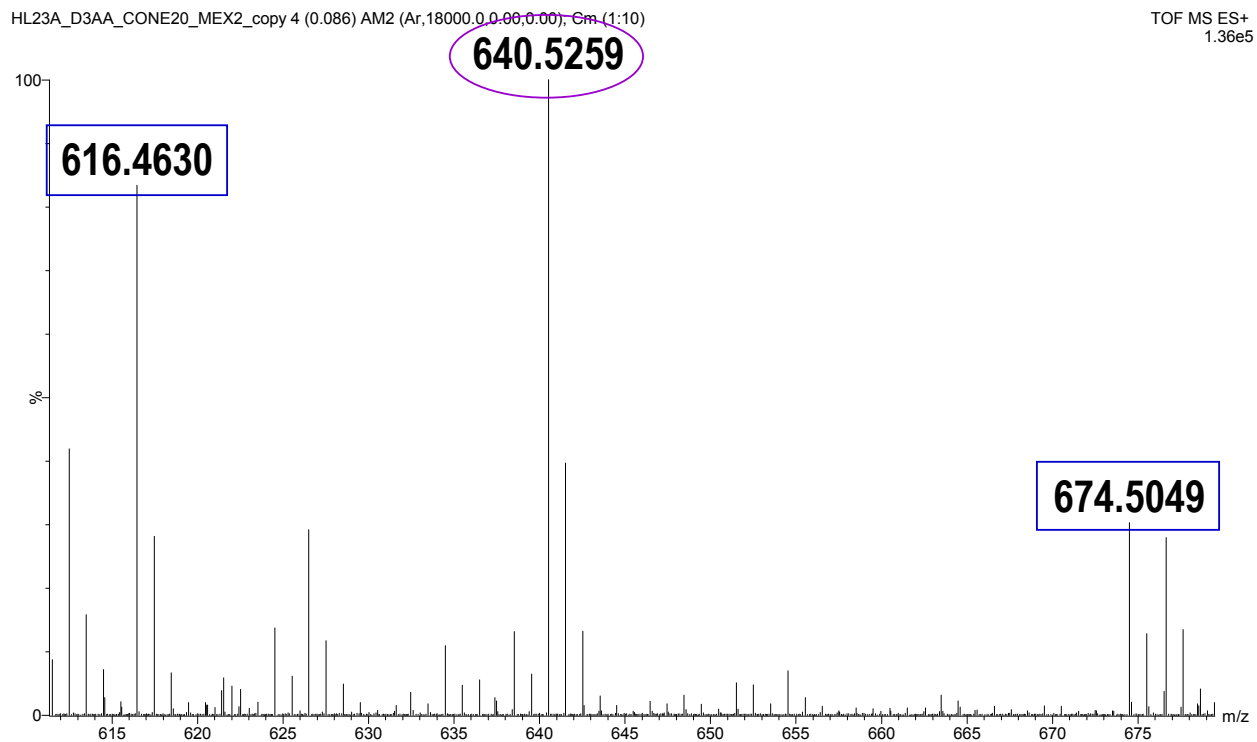


Figure S9: High resolution mass spectrum in electrospray positive mode of (Z)-bis(3-(dimethylamino)propyl)3,3'-((2(oleoyloxy)ethyl)azanediyl)dipropionate 7c (HL-23)



(The target ion is detected at m / z 640.5259 and the peaks retained for internal calibration are observed at m / z 616.4630 and m / z 674.5049, respectively)

Figure S10: ^1H NMR spectra of (Z)-bis(3(dimethylamino)propyl)3,3'((3(oleoyloxy)propyl)azanediyl)dipropanoate 7d, (HL-33)

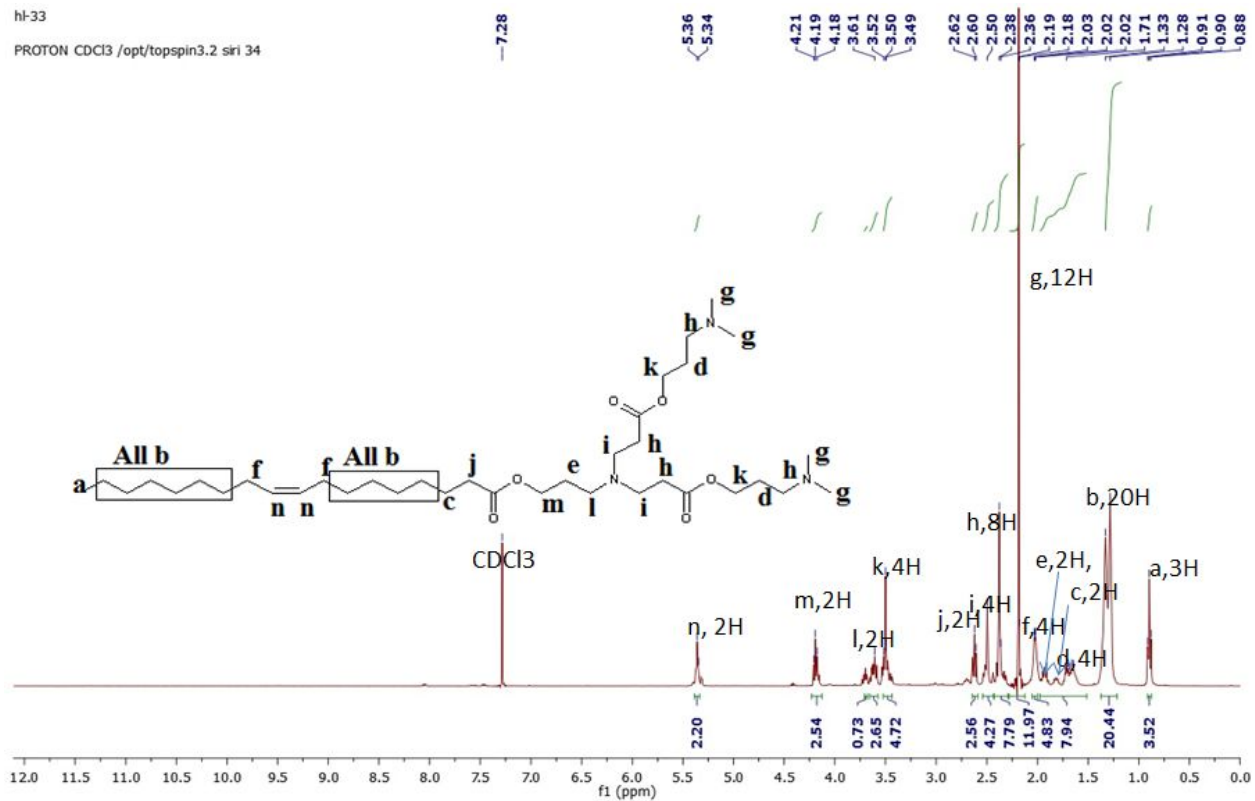
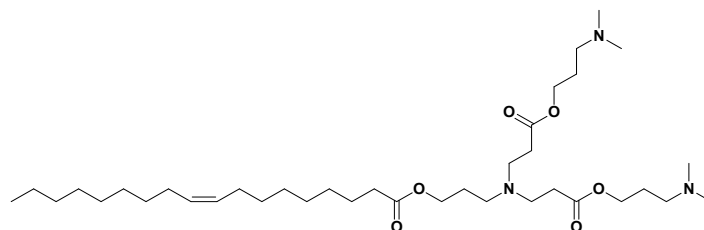


Figure S11: ^{13}C NMR spectra of (Z)-bis(3(dimethylamino)propyl)3,3'((3(oleoyloxy)propyl)azanediyl)dipropanoate 7d (HL-33)



(Z)-bis(3-(dimethylamino)propyl) 3,3'-((3-(oleoyloxy)propyl)azanediyl)dipropanoate

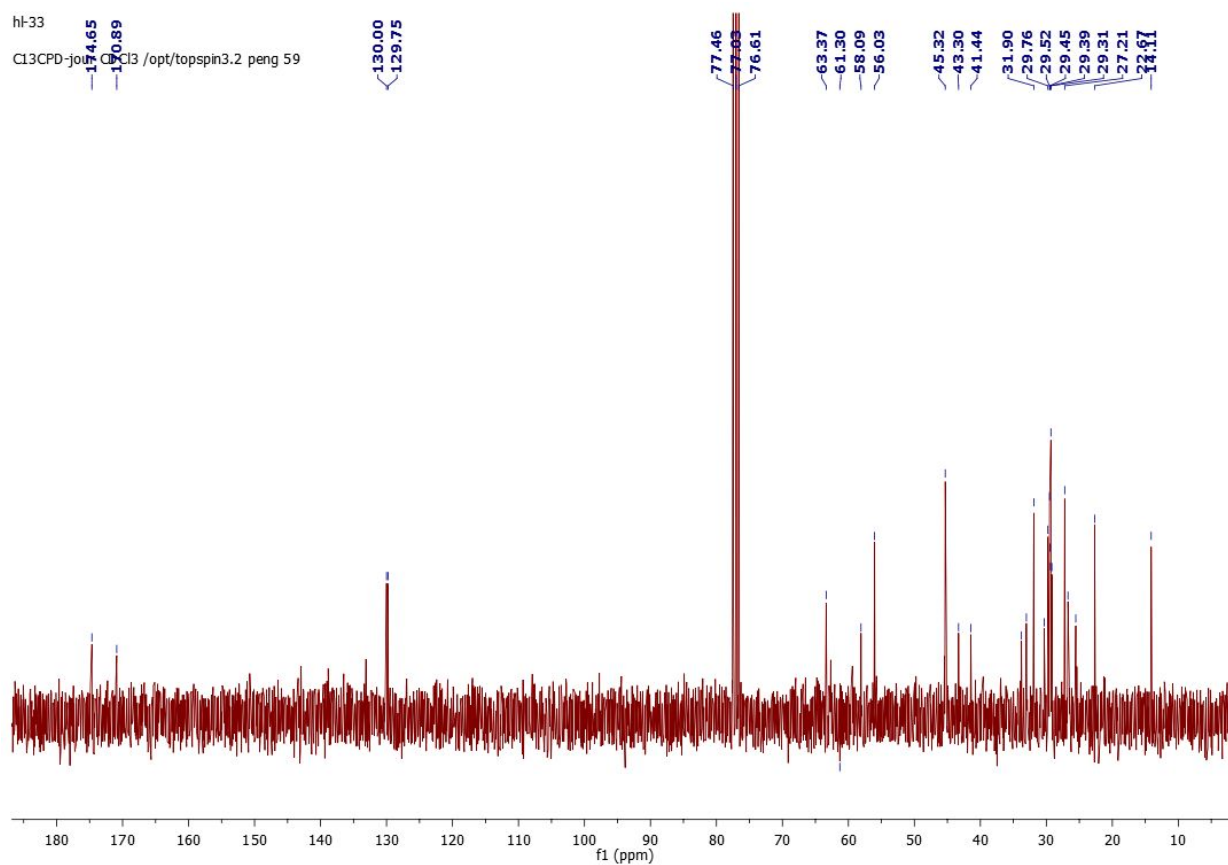
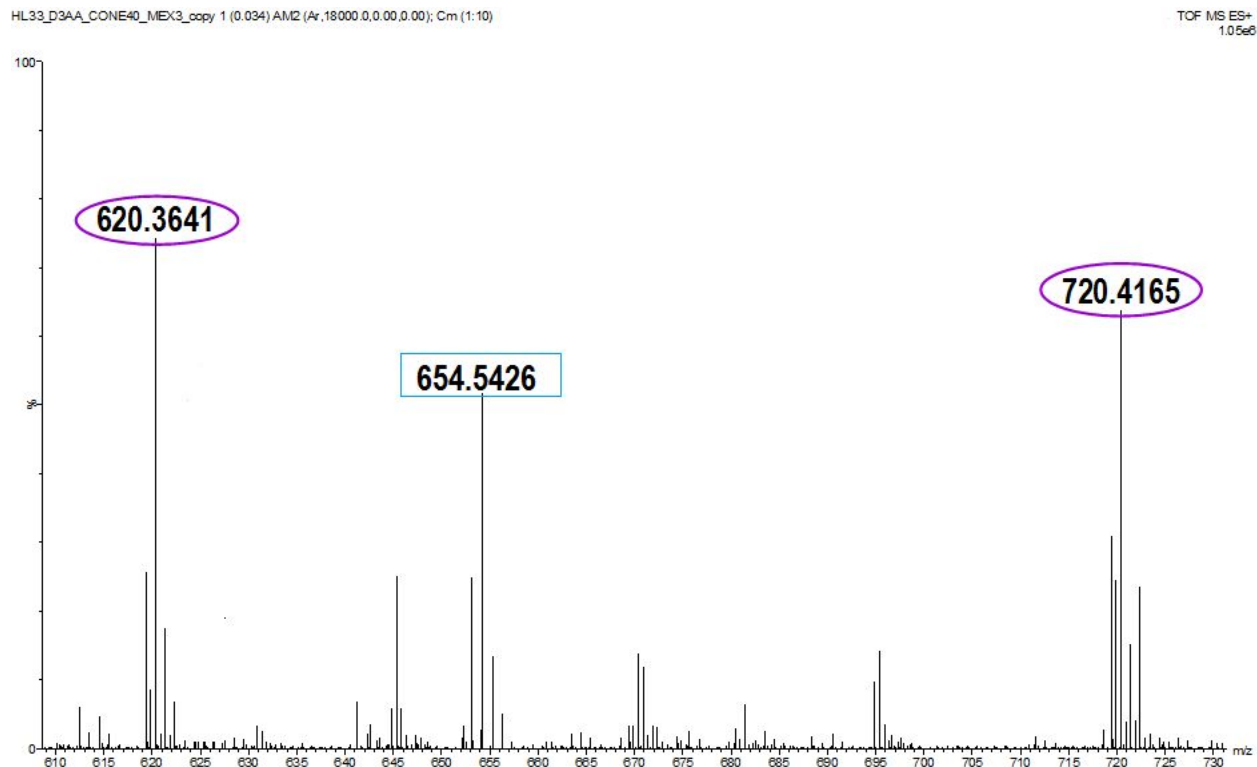


Figure S12: High resolution mass spectrum in electrospray positive mode of (Z)-bis(3(dimethylamino)propyl)3,3'((3(oleoyloxy)propyl)azanediyldipropanoate 7d (HL-33)



(The target ion is detected at m/z 654.5426 and the peaks retained for internal calibration are observed at m/z 620.3641 and m/z 720.4165 respectively)

Figure S13: ¹H NMR of (R)-2, 6-dioleamidohexanoic acid 10

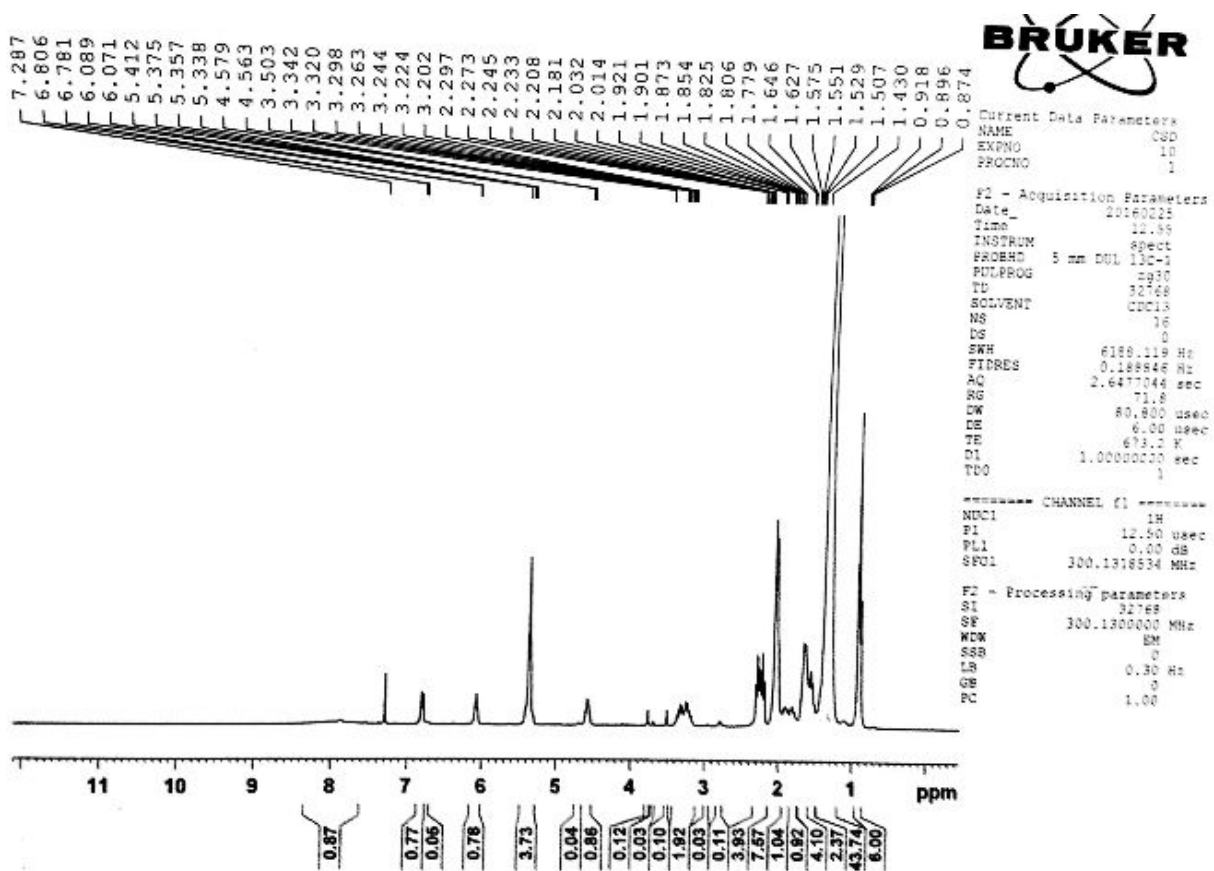
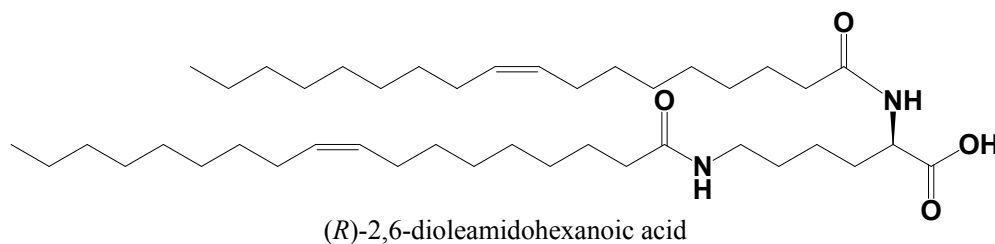


Figure S14: ¹³C NMR of (R)-2, 6-dioleamidohexanoic acid, 10

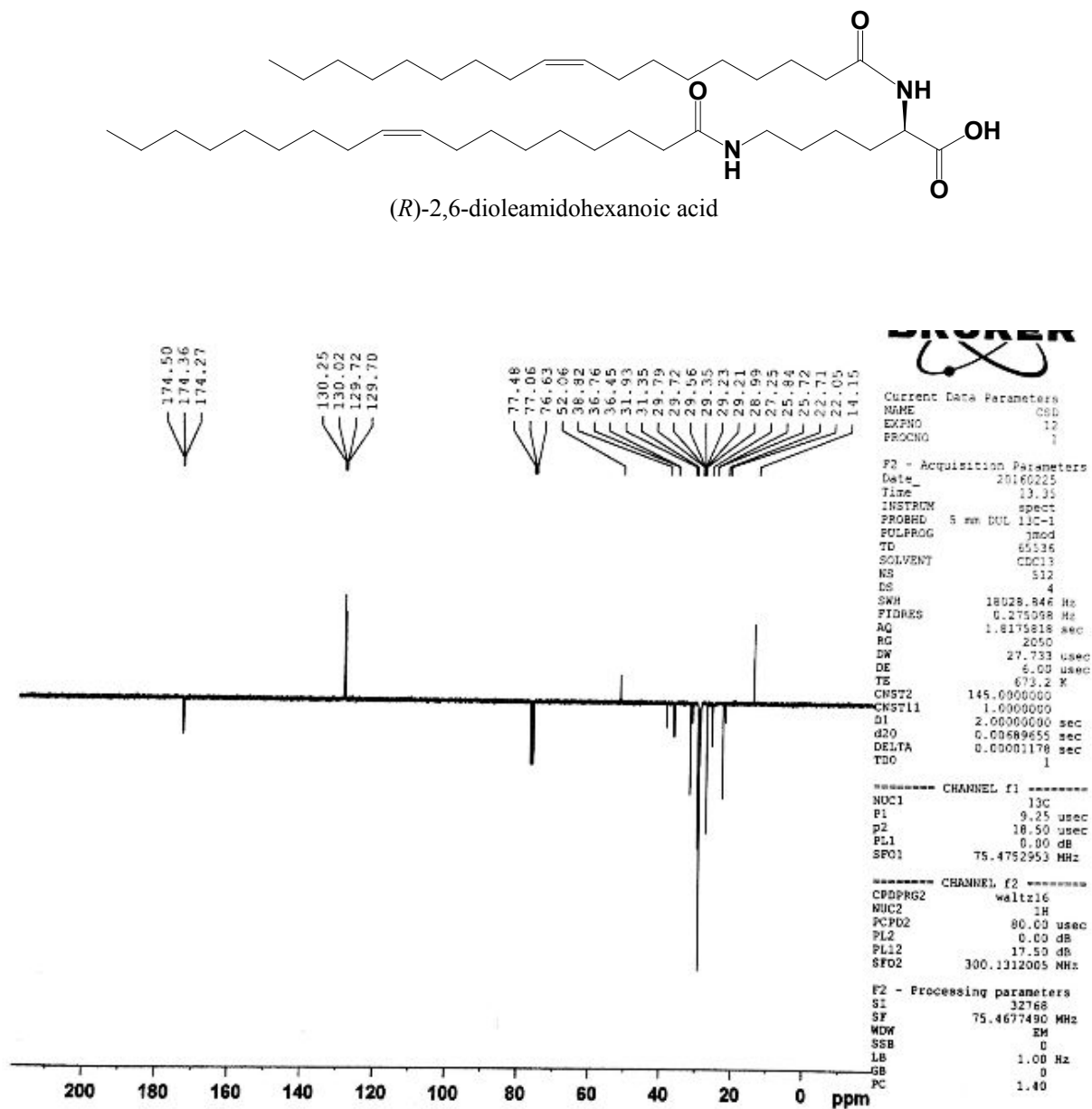


Figure S15: Mass of (R)-2, 6-dioleamidohexanoic acid, 10

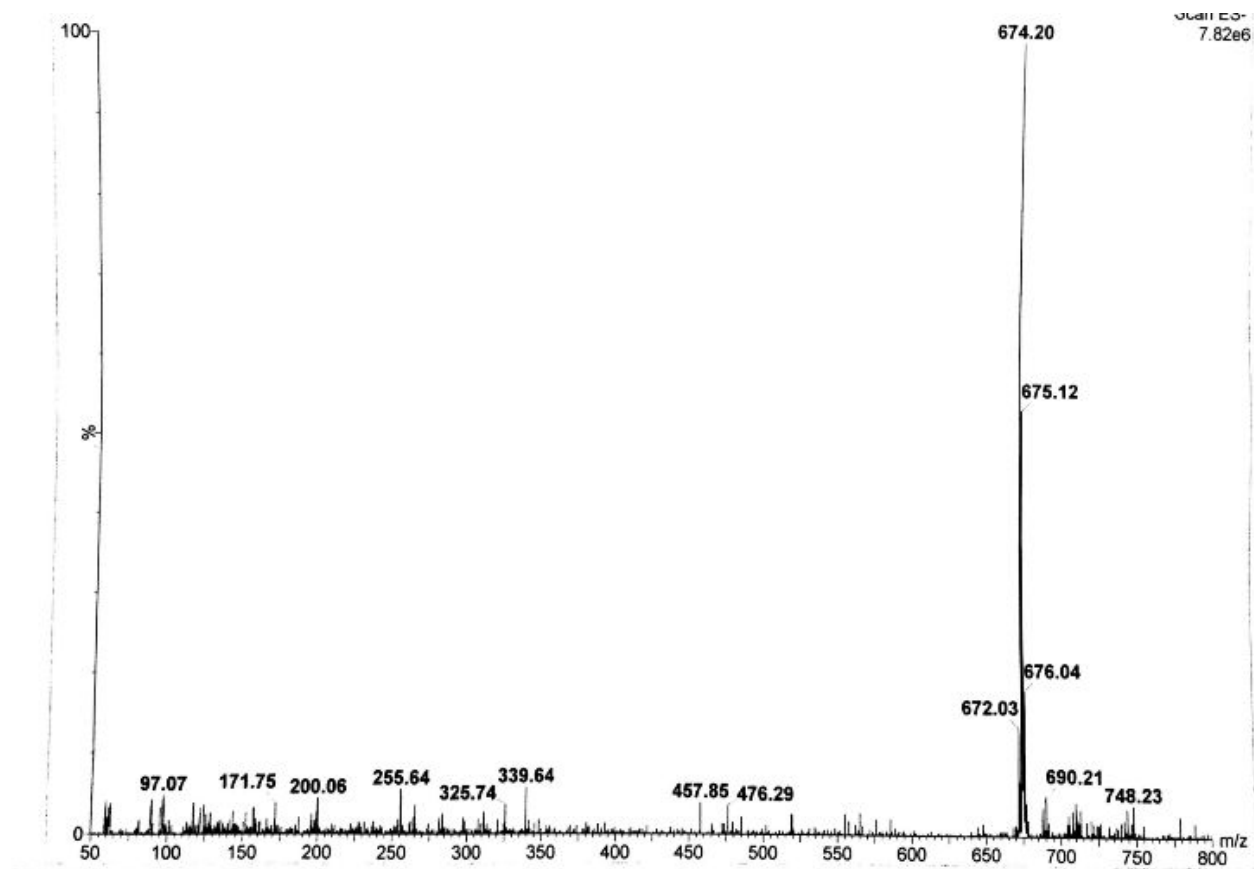


Figure S16: ¹H NMR (R)-2-(dimethylamino)ethyl 2,6-dioleamido hexanoate 12a (HLys E2)

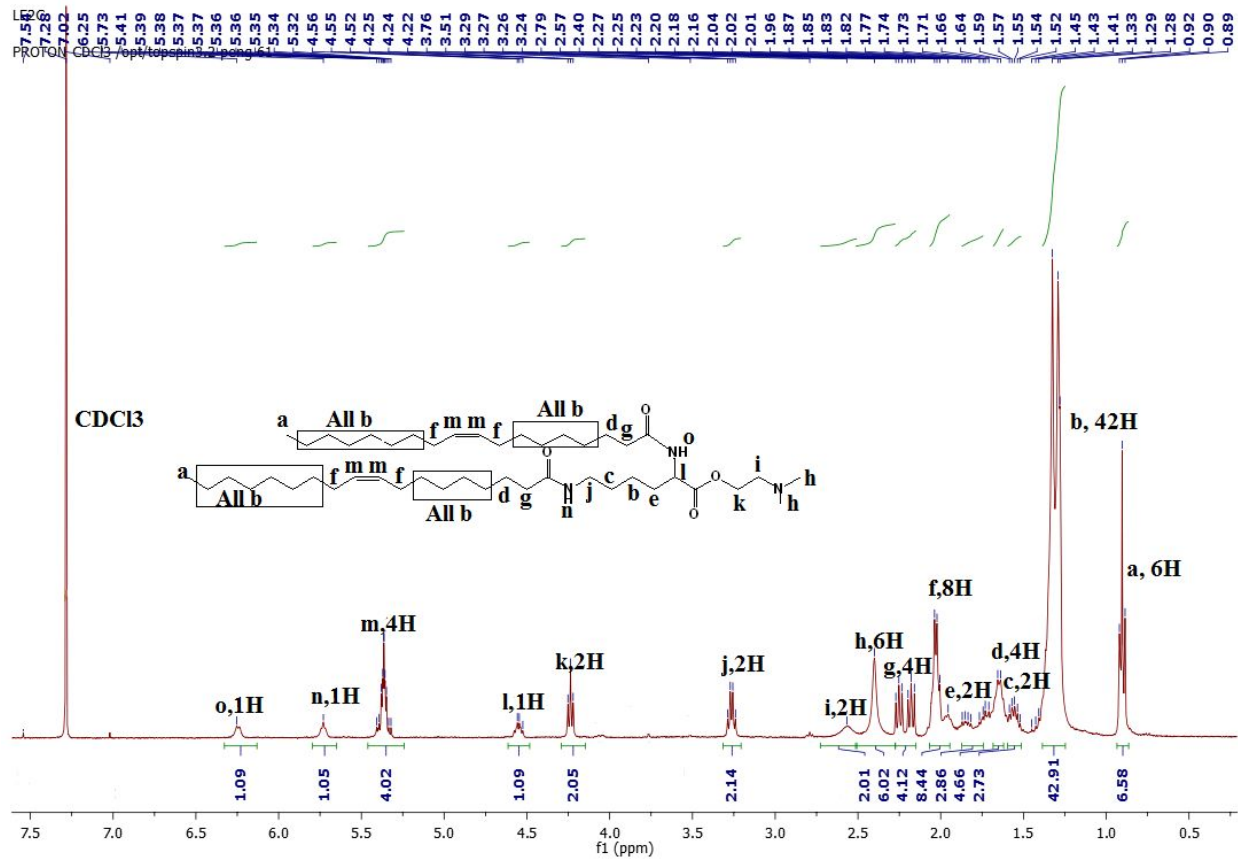


Figure S17: ^{13}C NMR (R)-2-(dimethylamino)ethyl 2,6-dioleamido hexanoate 12a (HLys E2)

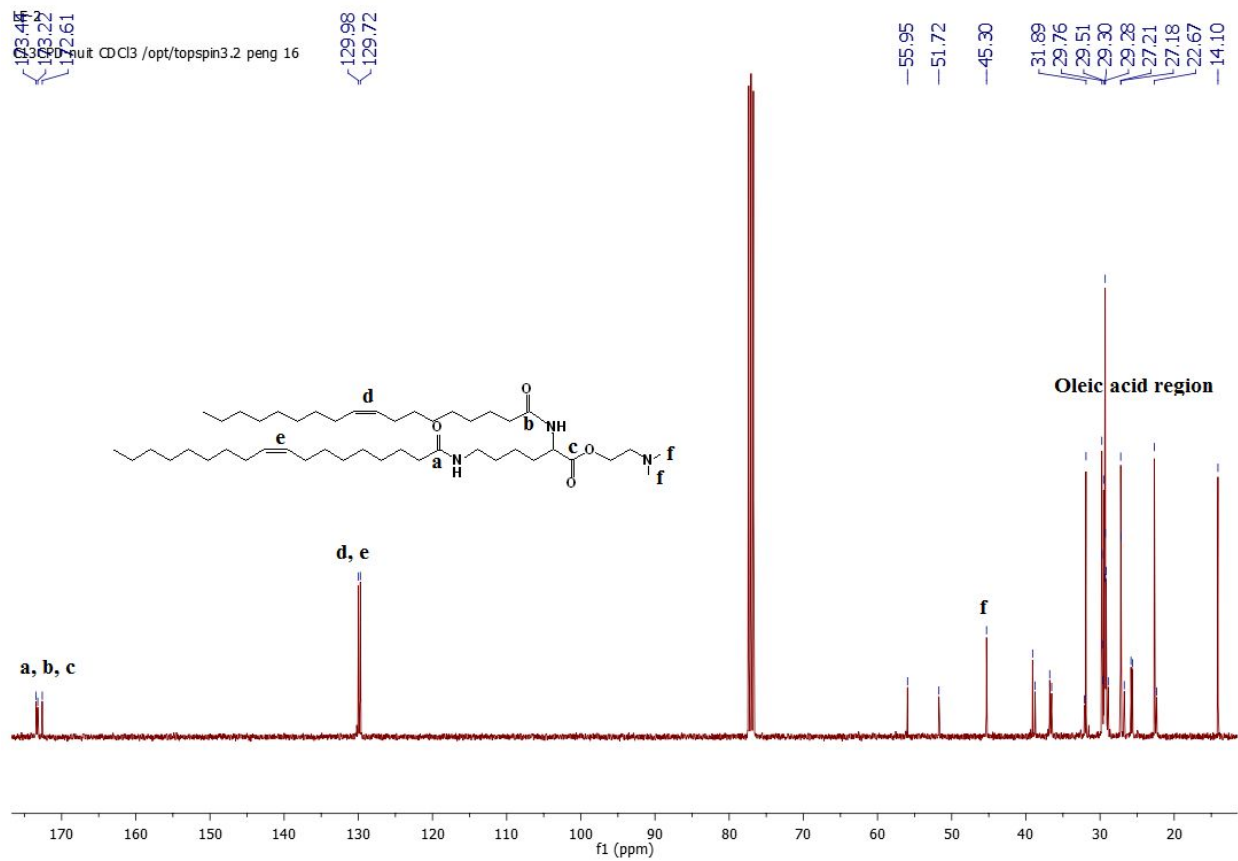
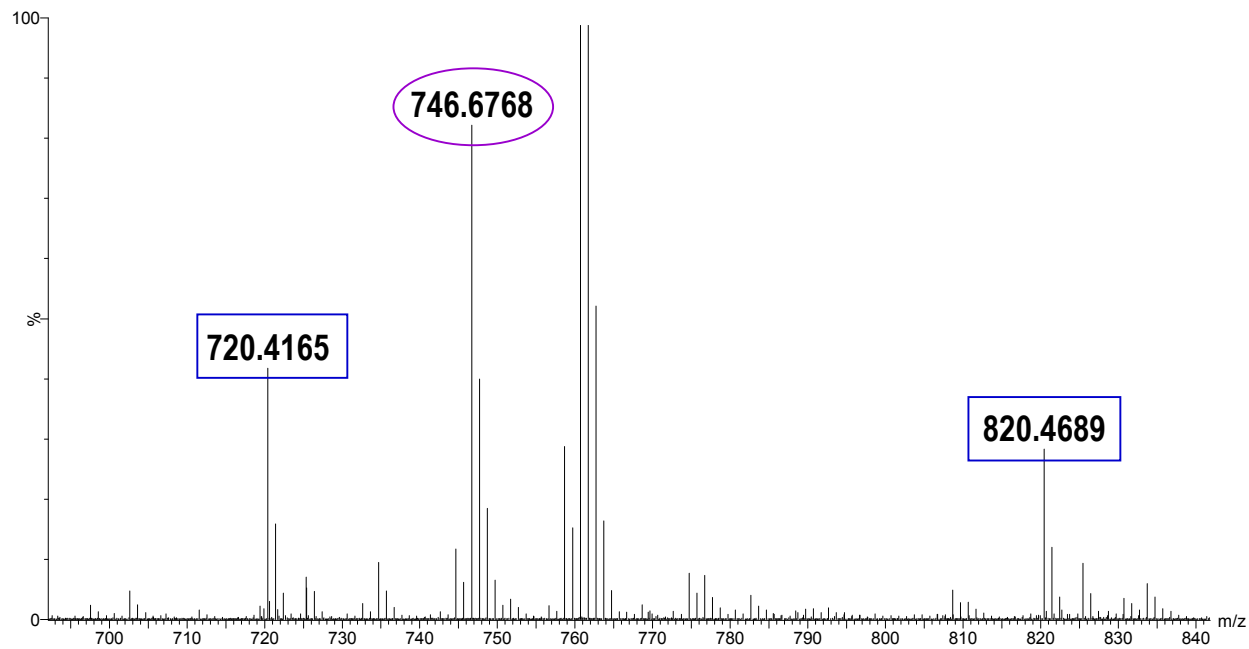


Figure S18: High resolution mass spectrum of (R)-2-(dimethylamino)ethyl 2,6-dioleamidohexanoate 12a (HLys E2).

LE2A_MEX2_copy 1 (0.034) AM2 (Ar,18000.0,0.00,0.00); Cm (1:10)

TOF MS ES+
5.90e5



(The target ion is detected at m/z 746.6768 and the peaks retained for internal calibration are observed at m/z 720.4165 and m/z 820.4689, respectively).

Figure S19: ^1H NMR (R)-3-(dimethylamino)propyl 2,6-dioleamidohexanoate 12b

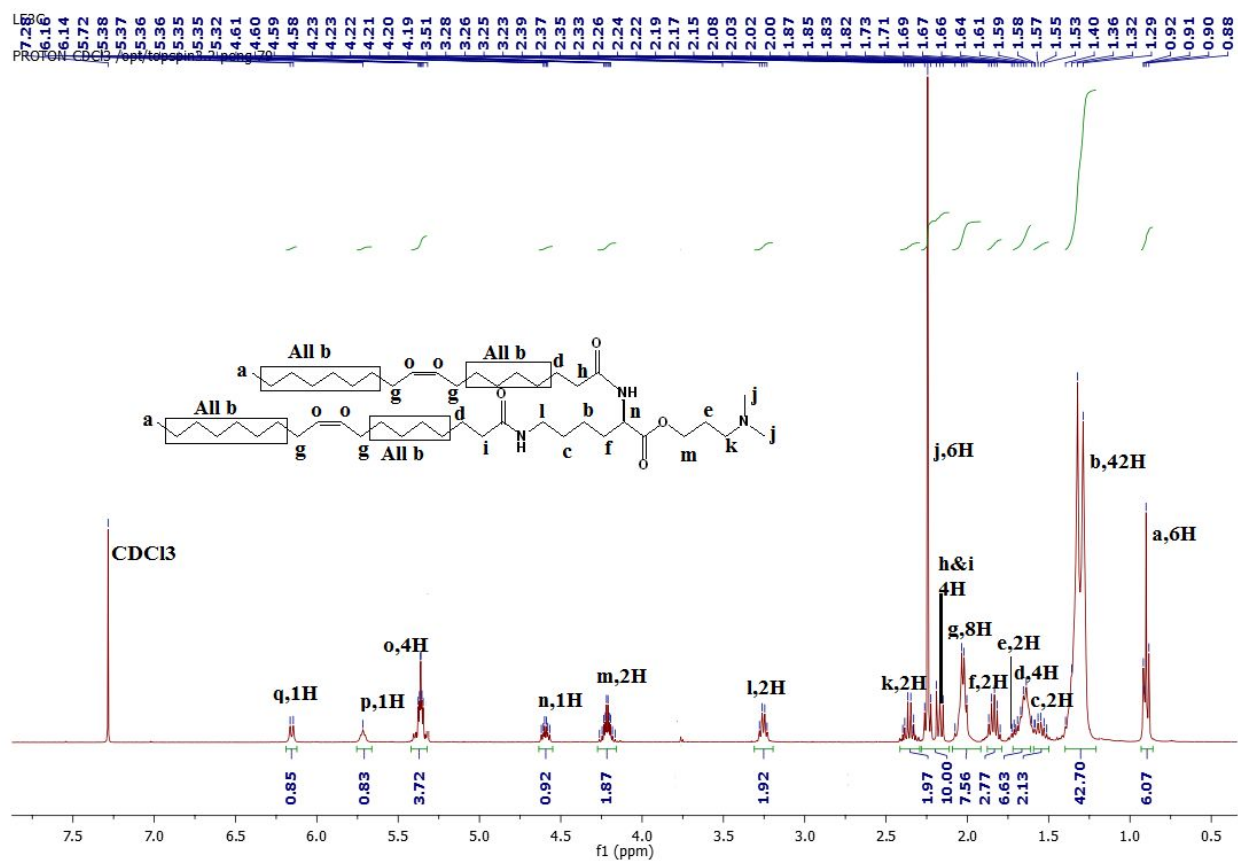


Figure S20: ^{13}C NMR (R)-3-(dimethylamino)propyl 2,6-dioleamido hexanoate 12b (HLys E3)

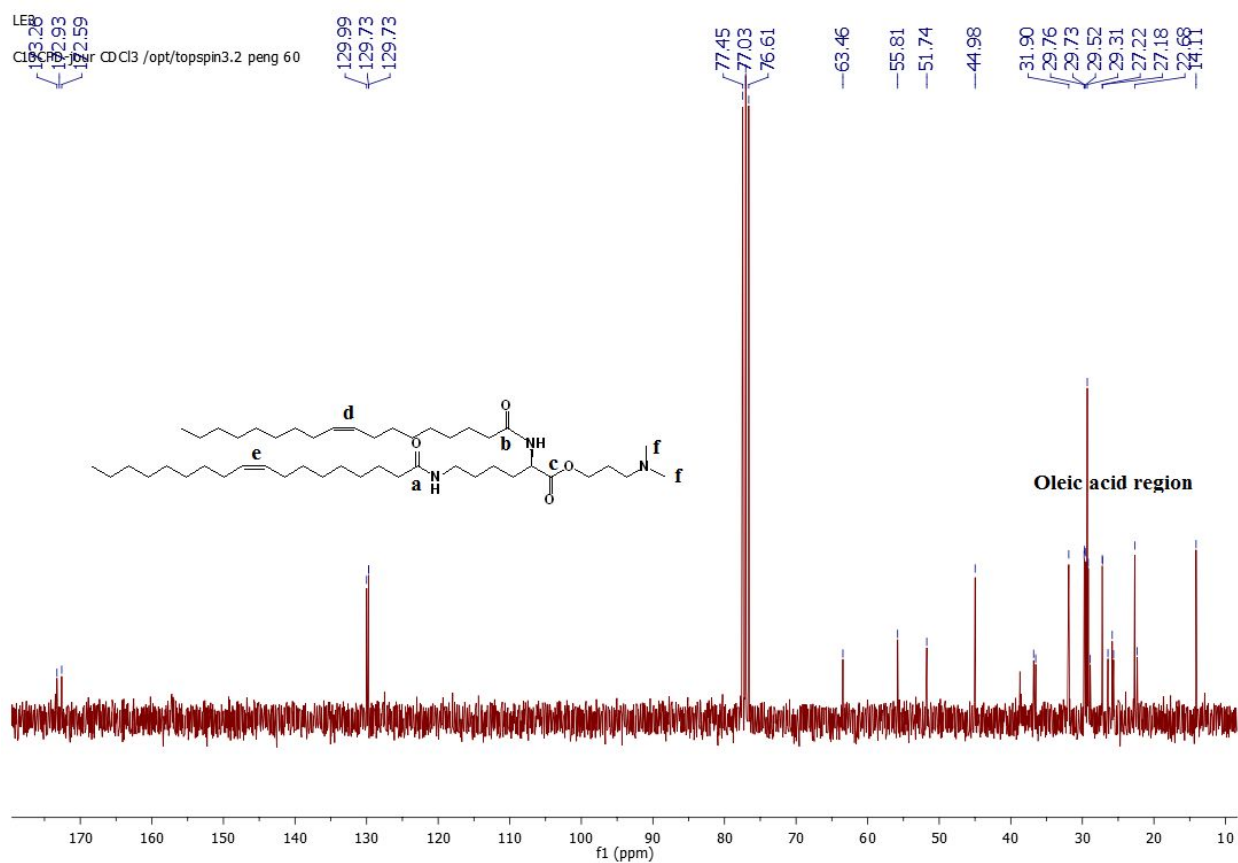
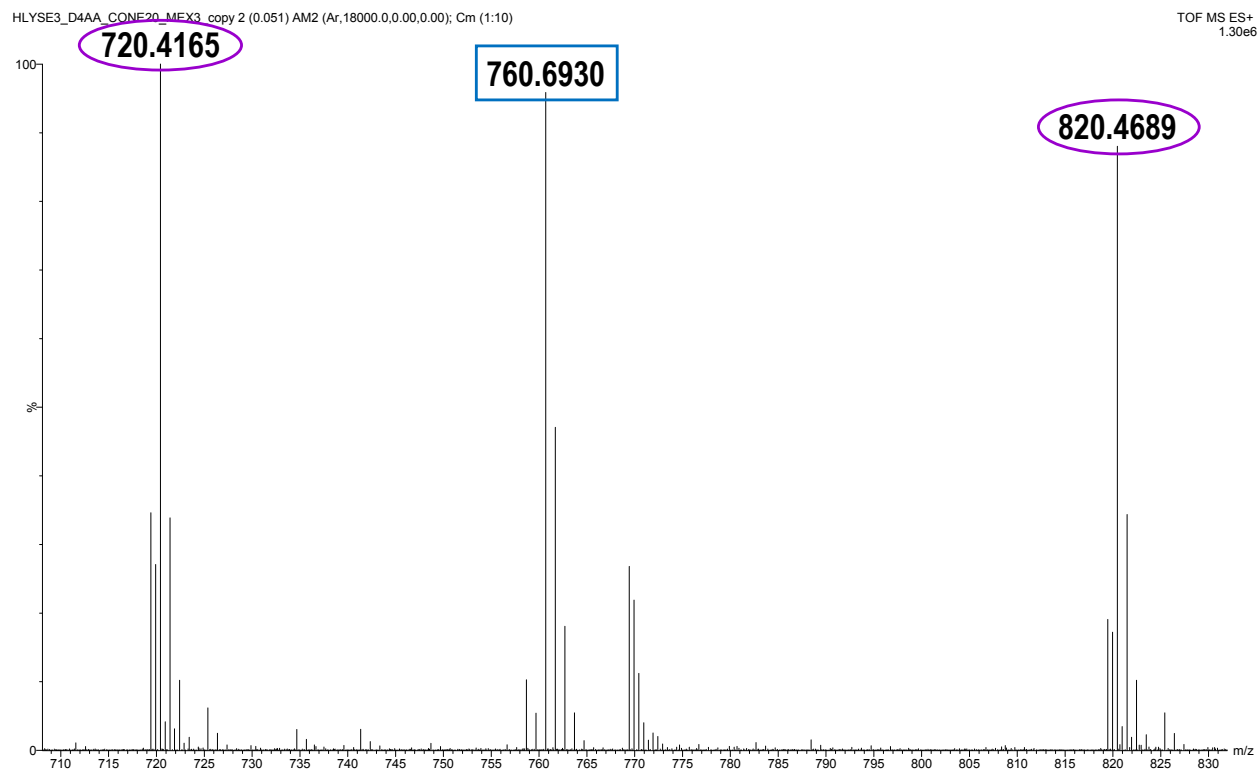


Figure S21: High resolution mass of (R)-3-(dimethylamino)propyl 2,6-dioleamidohexanoate 12b (HLys E3)



(The target ion is detected at m/z 760.6930 and the peaks retained for internal calibration are observed at m/z 720.4165 and m/z 820.4689 respectively)

Figure S22: ^1H NMR (*Z*)-*N,N'*-((*R*)-6-((2-(dimethylamino)ethyl)amino)-6-oxohexane-1,5-diyl)dioleamide 12c (HLys A2)

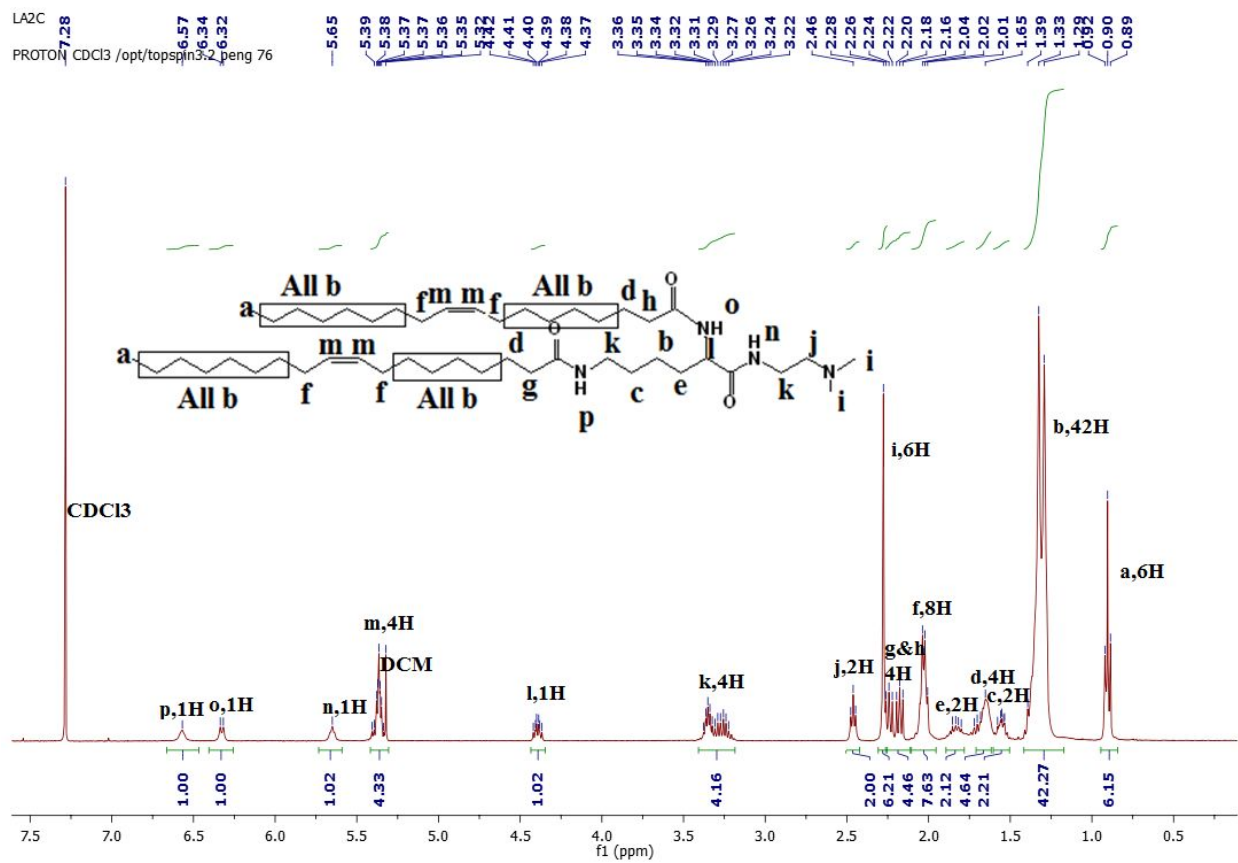


Figure S23: ^{13}C NMR (Z)-N,N'-((R)-6-((2-(dimethylamino)ethyl)amino)-6-oxohexane-1,5-diyl)dioleamide 12c (HLys A2)

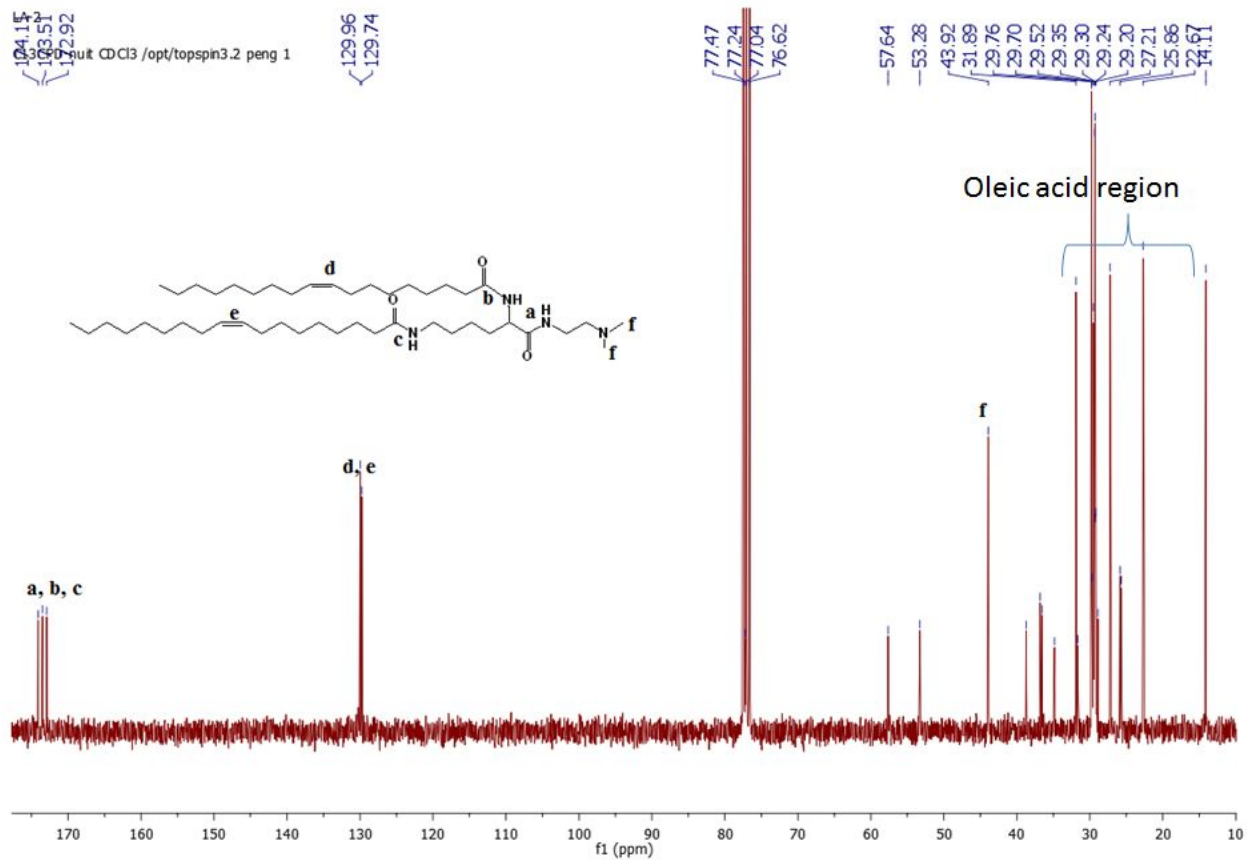
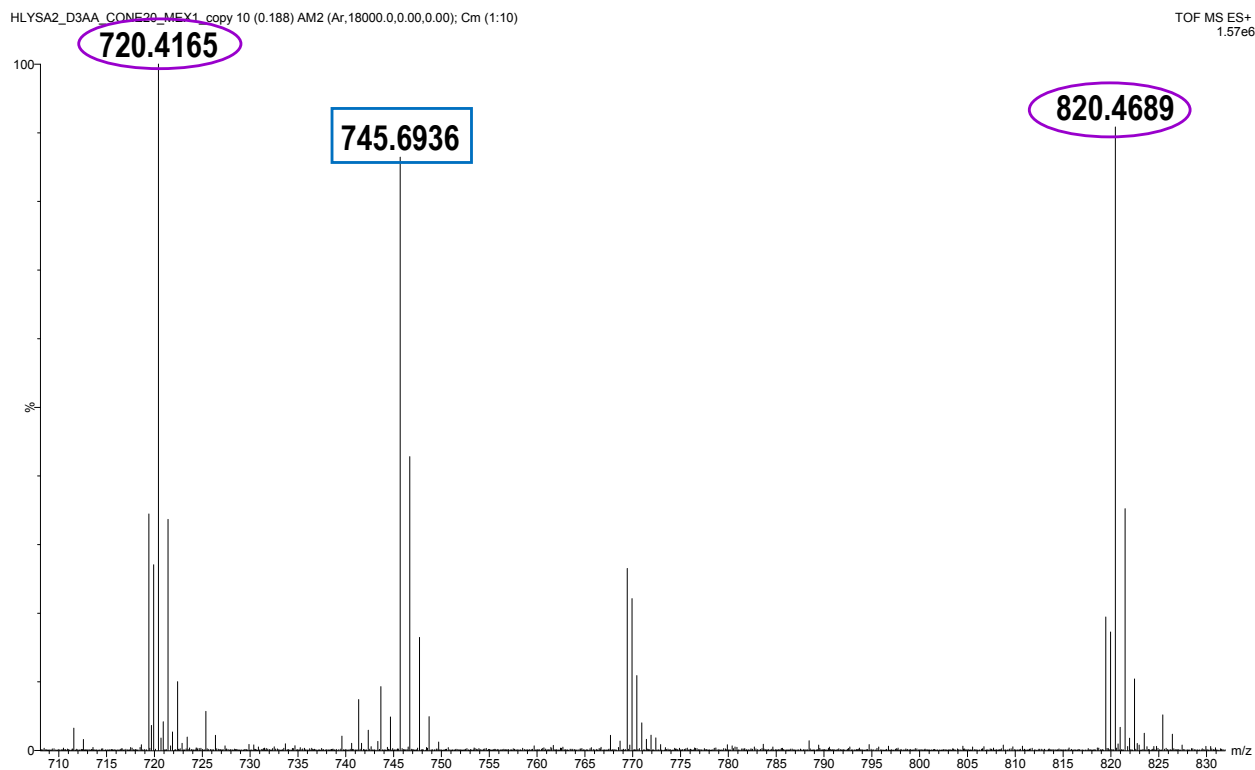


Figure S24: High resolution mass spectrum of (Z)-N,N'-((R)-6-((2-(dimethylamino)ethyl)amino)-6-oxohexane-1,5-diyl)dioleamide 12c (HLys A2)



(The target ion is detected at m/z 745.6936 and the peaks retained for internal calibration are observed at m/z 720.4165 and m/z 820.4689, respectively)

Figure S25: ^1H NMR (Z)-N,N'-((R)-6-((3-(dimethylamino)propyl)amino)-6-oxohexane-1,5-diyl)dioleamide 12d (HLysA3)

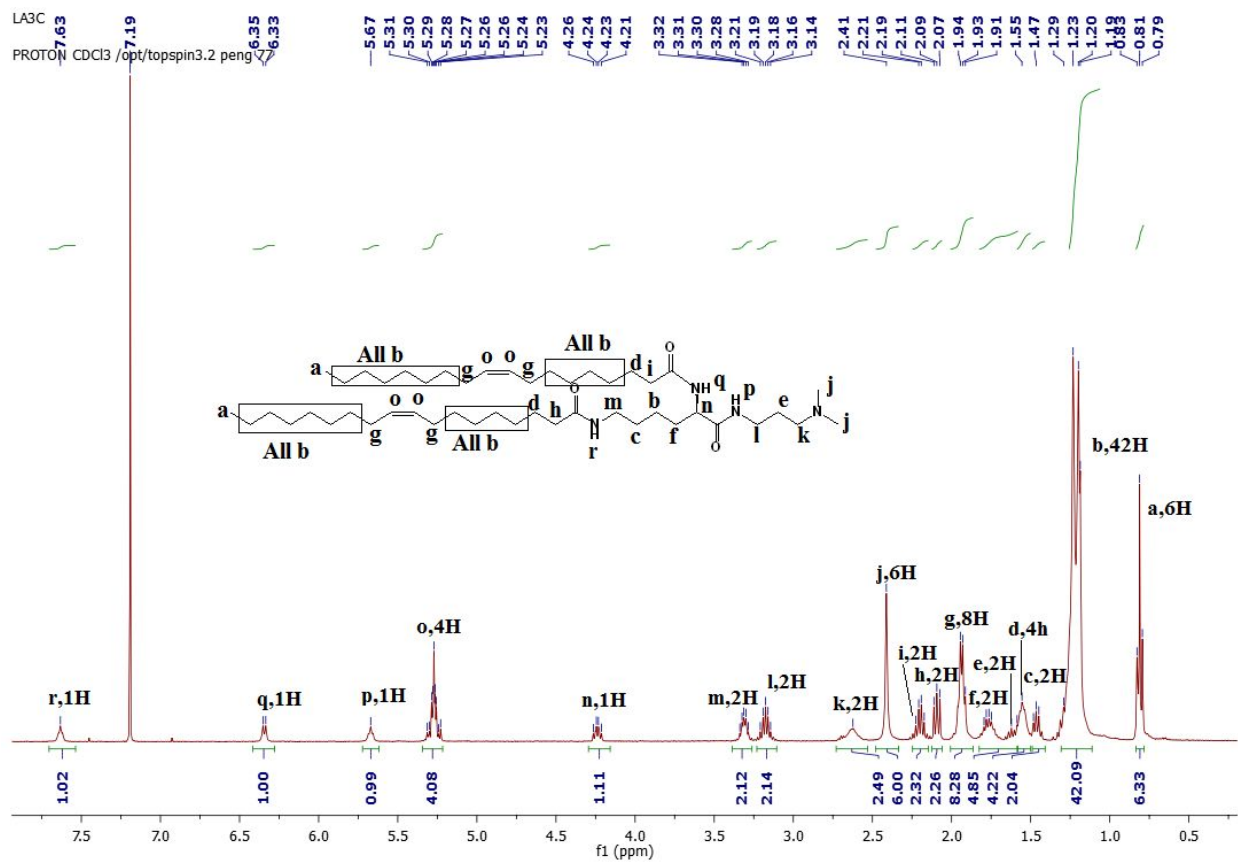


Figure S26: ^{13}C NMR (Z)-N,N'-((R)-6-((3-(dimethylamino)propyl)amino)-6-oxohexane-1,5-diyl)dioleamide 12d (HLysA3)

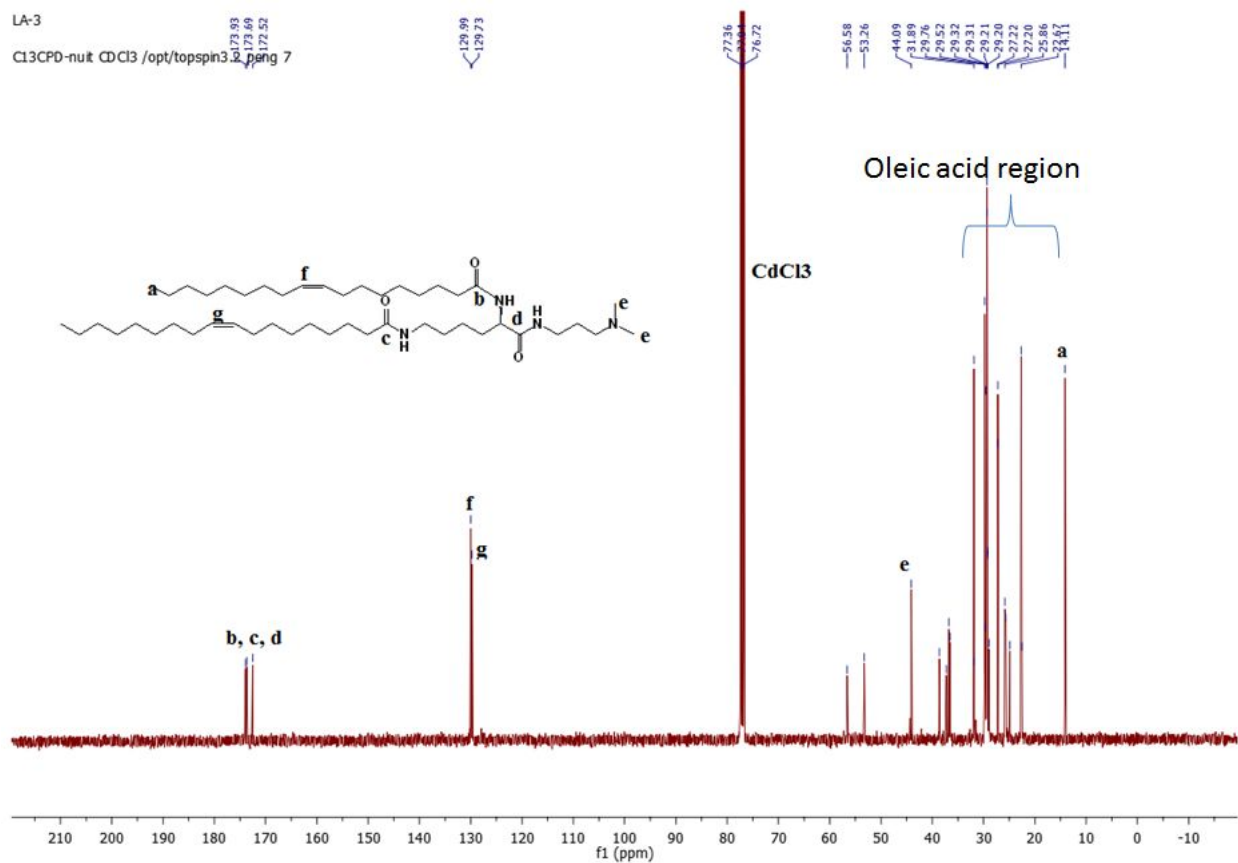
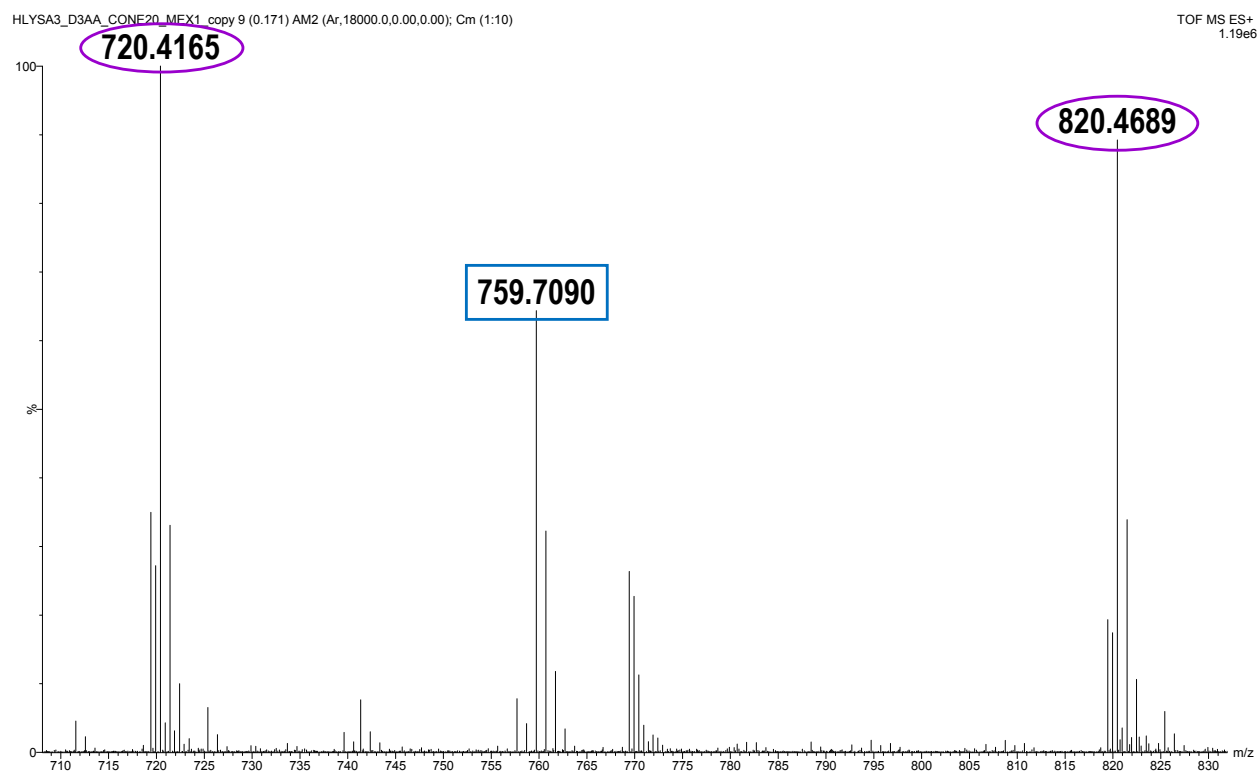


Figure S27: High resolution mass spectrum (Z)-N,N'-((R)-6-((3-(dimethylamino)propyl)amino)-6-oxohexane-1,5diyl)dioleamide 12d (HLysA3)



(The target ion is detected at m/z 759.7090 and the peaks retained for internal calibration are observed at m/z 720.4165 and m/z 820.4689, respectively)

Figure S28: Particle size of LNP'S

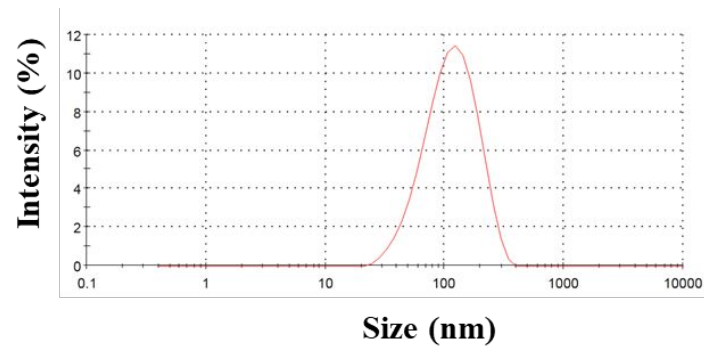
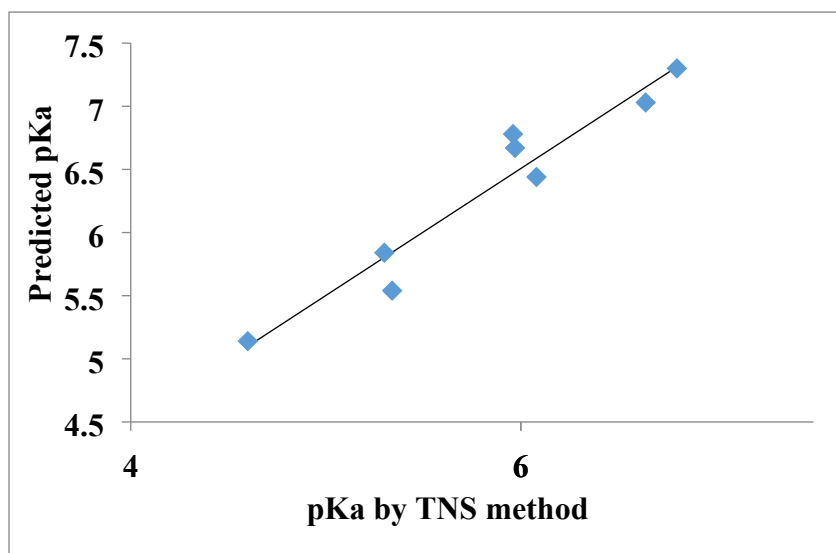


Figure S29: Correlation between predicted and experimental pKa



References

- S1 Bhadoriya, K. S.; Kumawat, N. K.; Bhavthankar, S. V.; Avchar, M. H.; Dhumal, D. M.; Patil, S. D.; Jain, S. V. Exploring 2D and 3D QSARs of benzimidazole derivatives as transient receptor potential melastatin 8 (TRPM8) antagonists using MLR and kNN-MFA methodology, *J. Saudi Chem. Soc.*, **2016**, *20*, S256-S270.
- S2 Geladi, P.; Kowalski, B. R. Partial least-squares regression: a tutorial. *Anal. Chim. Acta.* **1986**, *185*, 1-17.
- S3 Roy, K.; Kar, S.; Das, R. N. "Statistical methods in QSAR/QSPR," in A primer on QSAR/QSPR modeling, ed: Springer, **2015**, 37-59.
- S4 Alexander, G.; Alexander, T. Beware of Q2. *J Mol Graph Model* **2002**, *20*, 269-276.